Achieving Selectivity for Phosphate over Pyrophosphate in Ethanol with Iron(III)-Based Fluorescent Probes

Sheng-Yin Huang, Valérie C. Pierre*

Department of Chemistry, University of Minnesota, Twin-Cities, 207 Pleasant Street, SE, Minneapolis, MN 55455, USA

*Corresponding author: Valérie C. Pierre: pierre@umn.edu

Supporting Information

Table of Contents

Experimental Section

General considerations

Unless otherwise stated, all chemicals were purchased from commercial suppliers and used without further purification. Deuterated solvents were obtained from Cambridge Isotope Laboratories (Tewskbury, MA, USA). Distilled water was further purified by a Millipore Simplicity UV system (resistivity 18×10^6 Ω). All organic extracts were dried over anhydrous $MgSO_4$ (*s*). NaF, NaCl, NaBr, NaI, Na_2SO_4, $NaNO_3$, $NaHCO_3$, NaOAc**,** $Na_4P_2O_7$, and $Na_2HAsO_4\cdot7H_2O$ were used for anion screen studies. Flash chromatography was performed on Merck Silica Gel. Modified silica gel was prepared by heating the silica gel in 37% HCl (aq) at 50℃ for 6 h, further washing it with deionized water until the pH of the filtrate was neutral and drying it under reduced pressure at 100℃. The collected silica gel was subsequently suspended in toluene with 1% (v/v) hexadecyltrimethoxysilane. The mixture was stirred at 100°C for 6 h, after which the mixture was filtered, rinsed with toluene and ethyl acetate, and dried under reduced pressure at 100°C. ^{1}H NMR and ^{13}C NMR spectra were recorded at room temperature on a Bruker Advance III 400 at 400 MHz and 100 MHz, respectively, or a Bruker Advance III AV 500 at 500 MHz and 125 MHz, respectively, at the LeClaire-Dow instrumentation facility of the Department of Chemistry of the University of Minnesota. The residual solvent peaks were used as internal references. Data for ^{1}H NMR are recorded as follows: chemical shift (δ, ppm), multiplicity (s, singlet; d, doublet, t, triplet; q, quartet; br, broad; m, multiplet), coupling constant (Hz), integration. Data for ^{13}C NMR are recorded as follows: chemical shift (δ, ppm). Low resolution (LR) and high resolution (HR) electrospray spray ionization time-of-flight mass spectrometry (ESI/TOF-MS) were recorded on a Bruker BioTOF I at the LeClaire-Dow instrumentation facility of the Department of Chemistry of the University of Minnesota. UV-visible spectra were recorded on a Varian Cary 100 Bio Spectrophotometer. Data was collected over the range of 200 – 800 nm. Luminescence data was acquired on a Varian Cary Eclipse Fluorescence Spectrophotometer using a quartz cell with a path length of 1 cm and chamber volume 400 μL. Sample solutions were allowed to equilibrate for 5 min before measurement of their luminescence spectra, as initial studies demonstrated that this time was sufficient to achieve thermodynamic equilibrium (Figure S13 and Figure S14). All fluorescent titration data were acquired at room temperature (T = 25 ℃). Every data point was measured in triplicate from three independently prepared samples. For fluorescent titrations or anion selectivity studies, 5 mM of anions were prepared in water and pH adjusted to 7 using 0.1 N HCl or 0.1 N NaOH. Wet ethanol denotes the water content is ≤ 10 (v/v%) in ethanol. Luminescence data were processed with Scilab 6.0.2 and QtiPlot 0.9.8.9 software. All pH measurements were performed using Thermo Scientific Ag/AgCl refillable probe and a Thermo Orion 3 Benchtop pH meter. High-performance liquid chromatography (HPLC) data was collected on a Varian Prostar Model 210, coupled

with an Agilent ZORBAX Eclipse XDB-C18 column, and a Varian ProStar 335 diode array detector. Unless specified otherwise HPLC measurements were performed at a flow rate 1.0 mL min^{-1} with the following elution condition: 15% CH_3CN/85% water from 0 to 10 minutes, followed with a linear gradient to 85% CH_3CN/15% water from 10 to 23 minutes, 85% CH_3CN/15% water from 23 to 45 minutes.

Synthesis

4-nitrophenyl 1-(benzyloxy)-6-oxo-1,6-dihydropyridine-2-carboxylate (3). The *p*-nitrophenol activated ester was prepared in reference to a similar procedure for the preparation of *N*-hydroxysuccinimidyl ester of the podant.[1] HOPO(Bn)-OH (1000. mg, 4.080 mmol) was suspended in anhydrous methylene chloride (10 mL) under N_2 atmosphere, followed by the injection of oxalyl chloride (400. μL, 4.90 mmol) and one drop of DMF. The reaction was let stir for 1 hr at room temperature before the removal of solvent, HCl, and excess oxalyl chloride by high vacuum with liquid N_2 trap. Under N_2 atmosphere, the residue was dissolved in 10 mL anhydrous methylene chloride. After *p*-nitrophenol (568 mg, 4.08 mmol) was added to the solution, the mixture was cooled by ice bath, and NEt_3 (900 μL, 6.10 mmol) was injected slowly to the mixture. The mixture was then warmed up to room temperature for 6 hr, after which it was washed with 10% citric acid solution, 10% sodium bicarbonate solution, dried over anhydrous $MgSO_4$ (*s*), and concentrated under vacuum to a viscous liquid. This crude product was purified by flash chromatography over silica eluting with 60% EtOAc / 20% Hex to yield white solid **3** (1.363 g, 91 %). ^{1}H NMR (400 MHz, $CDCl_3$): δ 8.29 (d, J = 9 Hz, 2H), 7.49 (d, J = 6 Hz, 2H), 7.41-7.26 (m, 6H), 6.94 (d, J = 9 Hz, 1H), 6.79 (d, J = 7 Hz, 1H), 5.42 (s, 2H). ^{13}C NMR (100 MHz, $CDCl_3$): δ 158.6, 157.2, 154.4, 145.8, 137.1, 136.9, 133.3, 130.2, 129.4, 128.6, 127.6, 125.3, 122.2, 109.4, 78.8. ESI-HRMS: m/z = 389.0755 ($[M+Na]^+$), (Calcd. 389.0744).

***N*,*N*'-(azanediylbis(ethane-2,1-diyl))bis(1-(benzyloxy)-6-oxo-1,6-dihydropyridine-2-carboxamide) (4).** *p*-nitrophenol activated ester **3** (808 mg, 2.207 mmol) was dissolved in 20 mL methylene chloride, followed by slow injection of diethylenetriamine (119 μL, 1.10 mmol) and NEt_3 (300. μL, 2.21 mmol). The reaction was stirred at room temperature for 1 hr. The mixture was washed with 20 mL of 1N NaOH solution, dried over anhydrous $MgSO_4$ (*s*), and concentrated under vacuum to a viscous liquid. This crude product was purified by flash chromatography over silica eluting with 12% MeOH / 88% CH_2Cl_2 to yield foaming liquid **4** (1.045 g, 85 %). ^{1}H NMR (400 MHz, $CDCl_3$): δ 7.59 (br, 2H), 7.35-7.22 (m, 10H), 7.14 (dd, J_1 = 9 Hz, J_2 = 7 Hz, 2H), 6.36 (d, J = 9 Hz, 2H), 6.21 (d, J = 7 Hz, 2H), 5.18 (s, 4H), 3.14 (d, J = 10 Hz, 4H), 2.51-2.48 (m, 4H), 1.62 (br,1H). ^{13}C NMR (100 MHz, $CDCl_3$): δ 160.4, 158.3, 143.0, 138.3, 133.3, 129.6, 129.0, 128.3, 123.0, 105.6, 78.9, 47.1, 39.3. ESI-HRMS: m/z = 580.2156 ($[M+Na]^+$), (Calcd. 580.2167).

***N*,*N*'-(azanediylbis(ethane-2,1-diyl))bis(1-hydroxy-6-oxo-1,6-dihydropyridine-2-carboxamide) HBr (5).** The protected ligand **4** (200. mg, 0.359 mmol) was dissolved in 1 mL of glacial acetic acid, and 1 mL of 30% HBr was added to the reaction mixture. After 6 hr, acetic

acid and HBr were removed under high vacuum to yield a foaming liquid. This crude product was purified by flash chromatography over modified silica eluting with 0% MeOH / 100% H_2O gradient to 5% MeOH / 95% H_2O to yield white foaming liquid **5** (150 mg, 91%). ^{1}H NMR (400 MHz, CF_3COOD): δ 7.80 (t, J = 8 Hz, 2H), 7.52 (d, J = 8 Hz, 2H), 7.30 (d, J = 9 Hz, 2H), 4.00 (br, 4H), 3.65 (br, 4H). ^{13}C NMR (100 MHz, CF_3COOD): δ 165.4, 160.1, 141.4, 138.0, 121.9, 118.6, 51.6, 40.0. ESI-HRMS: m/z = 378.1310 ($[M-Br]^+$), (Calcd. 378.1408).

Fe^{III}-HOPO-fluo (1). Ligand **5** (5.0 mg, 0.011 mmol) and fluorescein (3.6 mg, 0.011 mmol) was suspended in anhydrous EtOH (10 mL), followed by injection of 1N NaOH (22 μL, 0.022 mmol). 0.1 N ethanolic $FeBr_3$ (110 μL, 0.011 mmol) was then added to the reaction mixture. The purity and identity of Fe^{III}-HOPO-fluo formed in situ were characterized by HPLC and ESI-HRMS. The solution was used without further purification. ESI-HRMS: m/z = 763.1138 ($[M-Br]^+$), (Calcd. 763.1208).

3-(2-(benzyloxy)phenyl)propanoic acid (6). The benzyl protected side arm **6** was synthesized according to the reported procedure[2] and characterized by NMR and ESI-HRMS. ^{1}H NMR (400 MHz, $CDCl_3$): δ 11.05 (br, 1H), 7.46-7.32 (m, 5H), 7.26-7.19 (m, 2H), 6.94-6.90 (m, 2H), 5.12 (s, 2H), 3.04 (t, J = 8 Hz, 2H), 2.72 (t, J = 8 Hz, 2H). ^{13}C NMR (100 MHz, $CDCl_3$): δ 179.6, 156.5, 137.2, 130.1, 128.8, 128.6, 127.8, 127.7, 127.0, 120.8, 111.6, 69.8, 34.0, 25.9. ESI-HRMS: m/z = 279.1009 ($[M+Na]^+$), (Calcd. 279.0992).

1-(benzyloxy)-*N*-(2-(*N*-(2-(1-(benzyloxy)-6-oxo-1,6-dihydropyridine-2-carboxamido)ethyl)-3-(2-(benzyloxy)phenyl)propanamido)ethyl)-6-oxo-1,6-dihydropyridine-2-carboxamide (7). The protected side arm **6** (316 mg, 1.23 mmol) was suspended in anhydrous methylene chloride (10 mL) under N_2 atmosphere, followed by the injection of oxalyl chloride (0.1 mL, 1.4 mmol) and one drop of DMF. The reaction was let stir for 1 hr at room temperature before the removal of solvent, HCl, and excess oxalyl chloride by high vacuum with liquid N_2 trap. Under N_2 atmosphere, the residue was dissolved in 10 mL anhydrous methylene chloride and cooled with ice bath. The protected ligand **4** (687 mg, 1.23 mmol) was dissolved in anhydrous methylene chloride (5 mL) and slowly injected to the cooled reaction mixture. To the mixture was then injected NEt_3 (344 μL, 2.47 mmol). The mixture was then warmed up to room temperature for 1 hr, after which it was washed with 10% citric acid solution, dried over anhydrous $MgSO_4$ (*s*), and concentrated under vacuum to a viscous liquid. This crude product was purified by flash chromatography over silica eluting with 4% MeOH / 96% CH_2Cl_2 to yield white foaming liquid **7** (805 mg, 82%). ^{1}H NMR (400 MHz, $CDCl_3$): δ 7.48-7.46 (m, 2H), 7.41-7.36 (m, 5H), 7.34-

7.27 (m, 9 H), 7.25-7.21 (m, 2H),7.13-7.09 (m, 2H), 6.94 (br, 1H), 6.89-6.82 (m, 3H), 6.68 (dd, J_1 = 1 Hz, J_2 = 8 Hz, 2H), 6.24 (t, J = 2 Hz, 1H), 6.23 (t, J = 2 Hz, 1H), 5.32 (s, 2H), 5.24 (s, 2H), 5.02 (s, 2H), 3.31 (br, 4H), 3.06 (br, 4H), 2.88 (t, J = 7 Hz, 2H), 2.48 (t, J = 8 Hz, 2H). ^{13}C NMR (100 MHz, $CDCl_3$): δ 174.3, 160.7, 160.6, 158.5, 158.4, 156.5, 142.8, 142.2, 138.0, 137.9, 137.0, 133.5, 133.1, 130.3, 130.1, 129.5, 129.1, 128.60, 128.55, 128.50, 128.0, 127.7, 127.3, 124.1, 120.8, 111.6, 105.9, 105.2, 79.3, 79.0, 69.9, 47.40, 45.7, 39.3, 38.7, 32.8, 26.9. ESI-HRMS: m/z = 818.3181 ($[M+Na]^+$), (Calcd. 818.3160).

1-hydroxy-*N*-(2-(*N*-(2-(1-hydroxy-6-oxo-1,6-dihydropyridine-2-carboxamido)ethyl)-3-(2-hydroxyphenyl)propanamido)ethyl)-6-oxo-1,6-dihydropyridine-2-carboxamide (8). The protected ligand **7** (450. mg, 0.566 mmol) was dissolved in 1 mL of glacial acetic acid, and 1 mL of 30% HBr was added to the reaction mixture. After 6 hr, acetic acid and HBr were removed under high vacuum to yield a foaming liquid. This crude product was purified by flash chromatography over modified silica eluting with 0% MeOH / 100% H_2O gradient to 5% MeOH / 95% H_2O to yield white foaming liquid **8** (270 mg, 91%). ^{1}H NMR (500 MHz, CD_3OD): δ 7.48-7.42 (m, 2H), 7.04 (d, J = 7 Hz, 1H), 6.97 (dd, J_1 = 1 Hz, J_2 = 8 Hz, 2H), 6.75-6.68 (m, 4H), 6.61 (dd, J_1 = 1 Hz, J_2 = 7 Hz, 1H), 6.56 (dd, J_1 = 1 Hz, J_2 = 7 Hz, 1H), 3.65-3.61 (m, 4H), 3.56-3.54 (m, 4H), 2.88 (t, J = 7 Hz, 2H), 2.75 (t, J = 8 Hz, 2H). ^{13}C NMR (125 MHz, CD_3OD): δ 176.5, 162.8, 162.7, 160.2, 160.1, 156.5, 142.0, 141.7, 139.0, 138.8, 131.5, 128.7, 120.94, 120.85, 116.4, 108.7, 108.5, 48.3, 46.3, 39.4, 39.0, 34.7, 27.6. ESI-HRMS: m/z = 524.1775 ($[M-H]^-$), (Calcd. 524.1776).

Fe^{III}-HOPO-PhO-fluo (2). Ligand **8** (5.0 mg, 9.5 μmol) and fluorescein (3.6 mg, 9.5 μmol) was suspended in anhydrous EtOH (10 mL), followed by injection of 1N NaOH (29 μL, 29 μmol). 0.1 N ethanolic $FeBr_3$ (95 μL, 9.5 μmol) was then added to the reaction mixture. The purity and identity of Fe^{III}-HOPO-PhO-fluo formed in situ were characterized by HPLC and ESI-HRMS. The solution was used without further purification. ESI-HRMS: m/z = 911.1830 ($[M+3H]^+$), (Calcd. 911.1733).

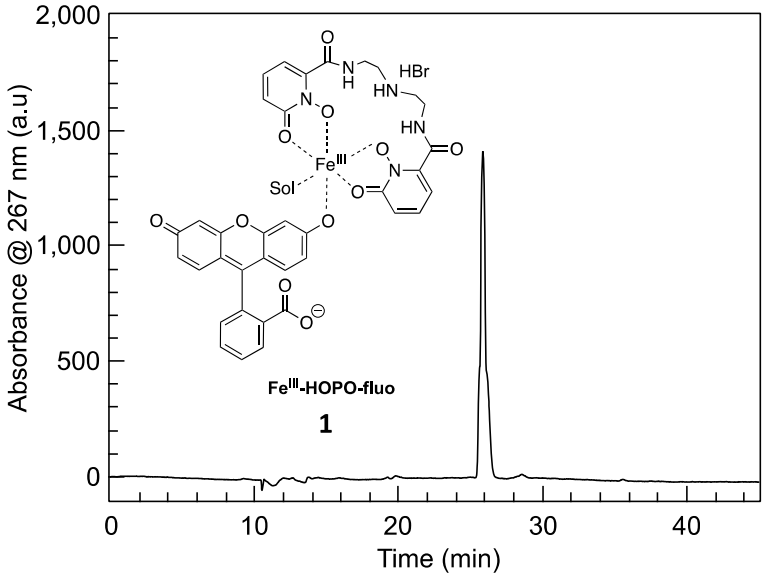

Figure S1. HPLC chromatogram of Fe^{III}-HOPO-fluo **(1)**.

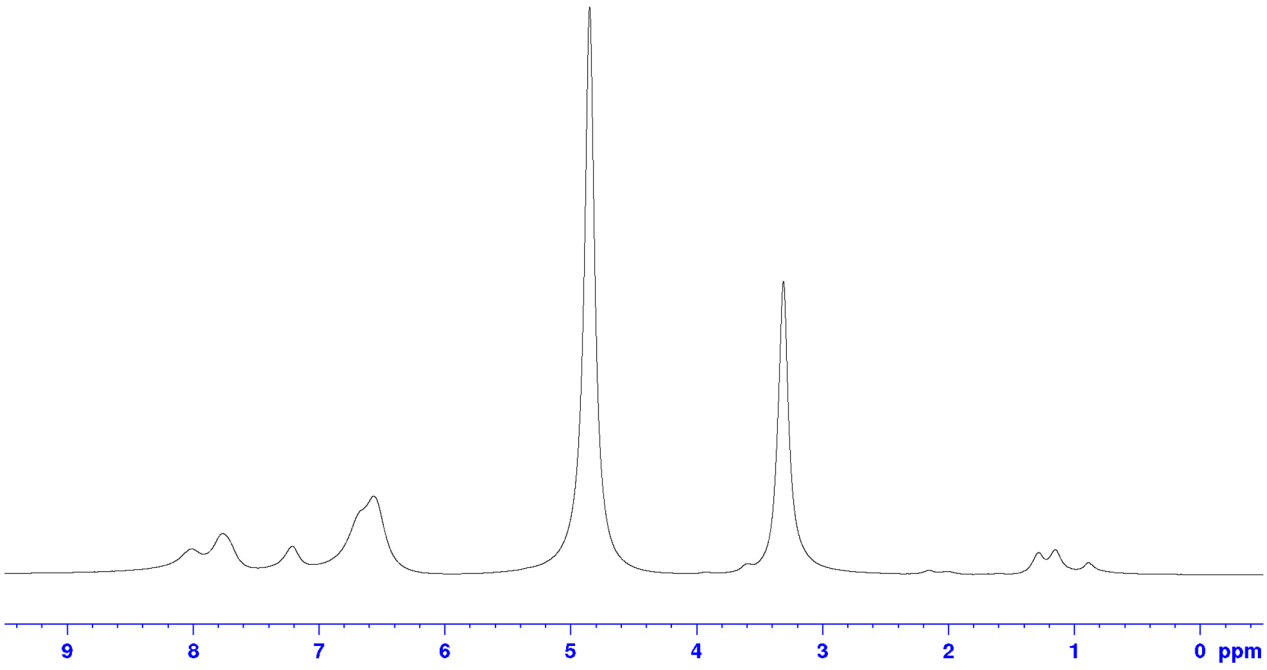

Figure S2. ^{1}H NMR spectrum of Fe^{III}-HOPO-fluo (**1**, CD_3OD, 400 MHz).

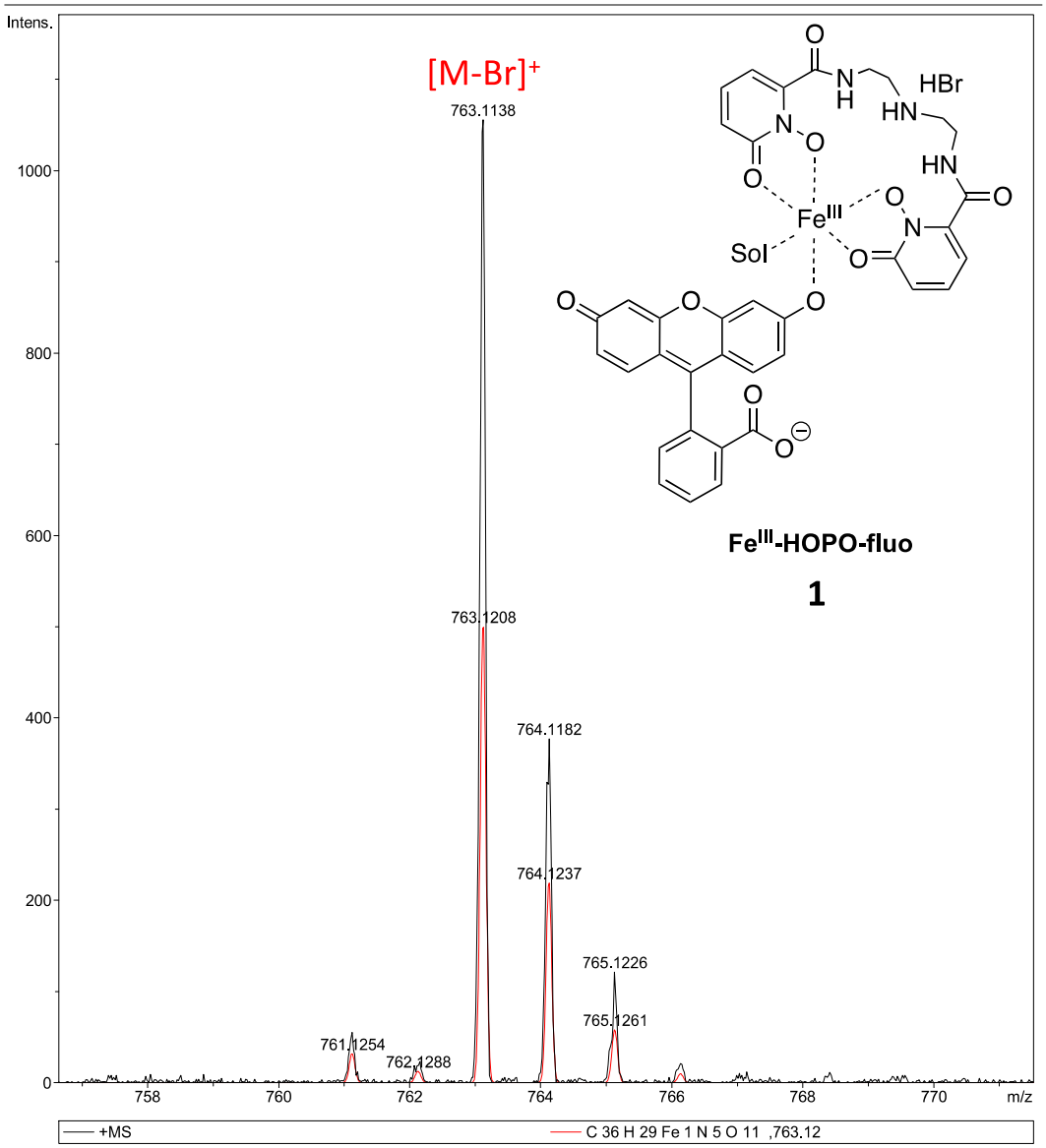

Figure S3. Experimental (black) and calculated (red) ESI-MS spectrum of Fe^{III}-HOPO-fluo (**1**).

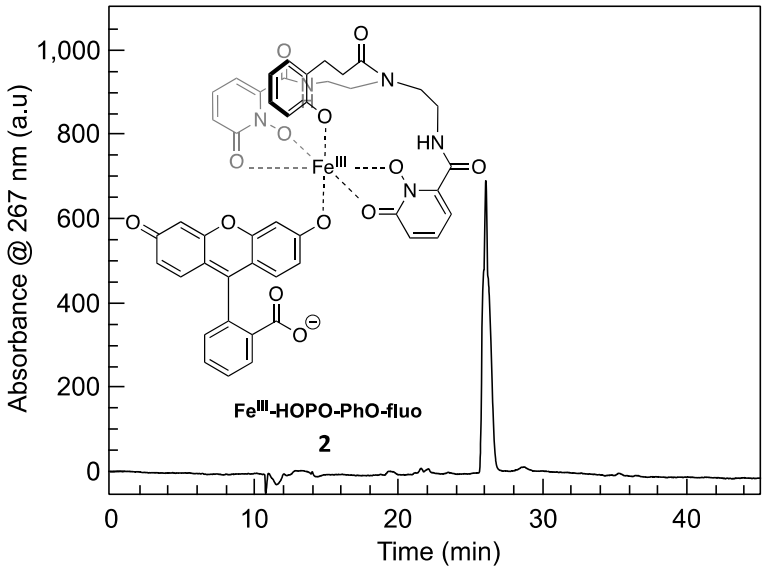

Figure S4. HPLC chromatogram of Fe^{III}-HOPO-PhO-fluo (**2**).

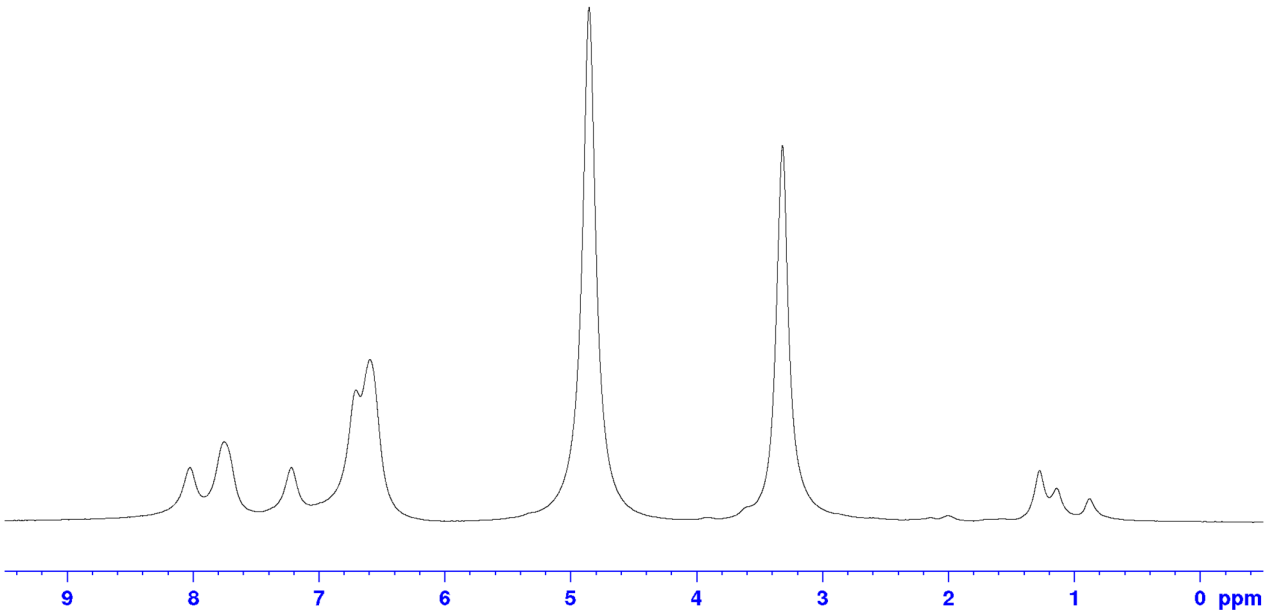

Figure S5. ^{1}H NMR spectrum of Fe^{III}-HOPO-Ph-fluo (**2,** CD_3OD, 400 MHz).

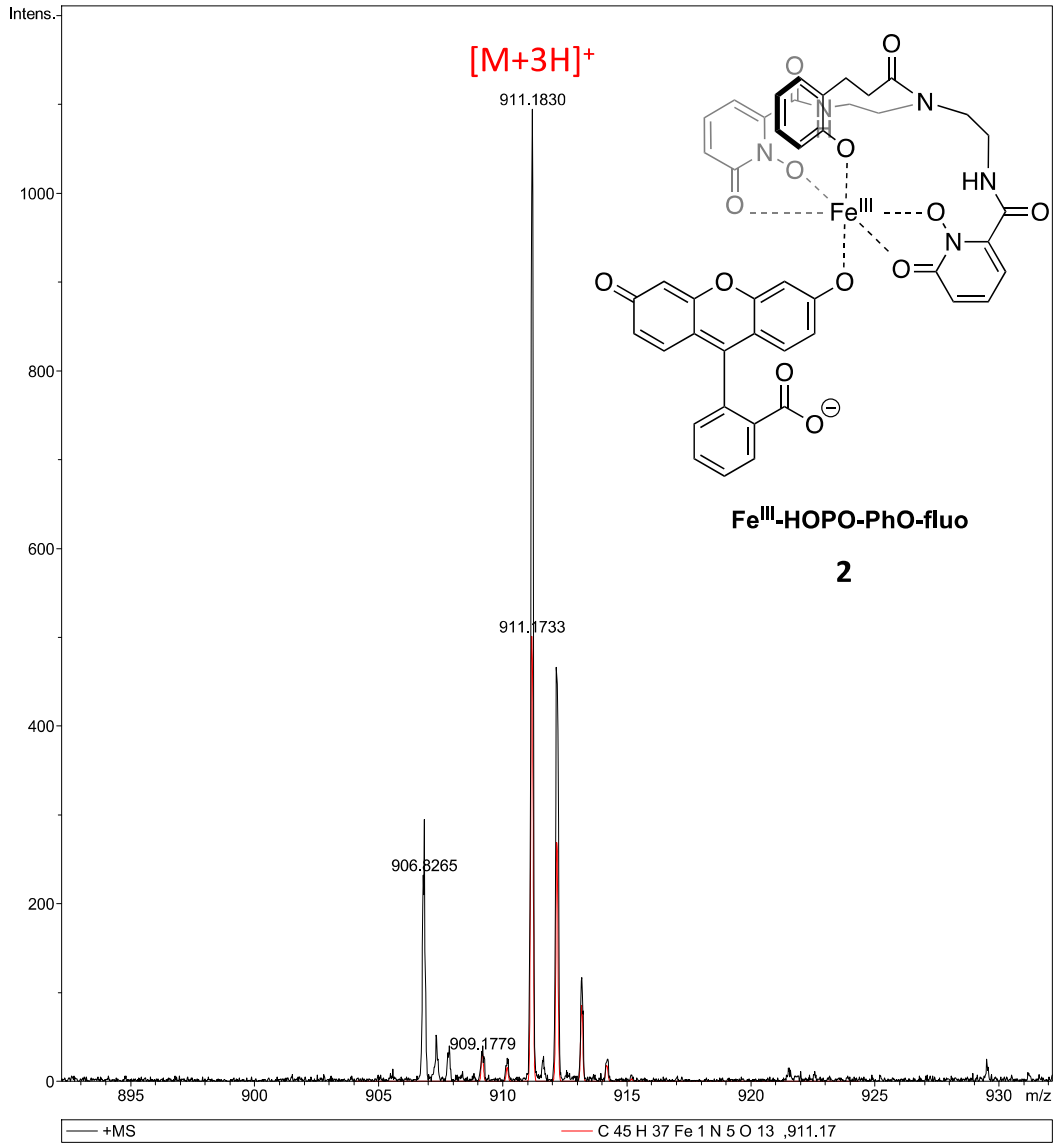

Figure S6. Experimental (black) and calculated (red) ESI-MS spectrum of Fe^{III}-HOPO-PhO-fluo (**2**). Note the peak at 906.8265 m/z came from PPG calibrant for obtaining the high-resolution MS spectrum.

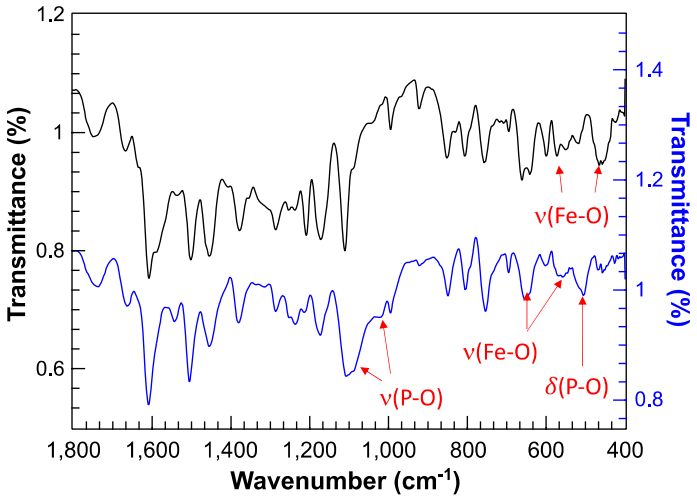

Figure S7. ATR-IR spectra of Fe^{III}-HOPO-PhO-fluo complex in the presence and absence of 1eq. phosphate. Sample preparations: to the ethanolic Fe^{III} complex solution was added equimolar phosphate. The pH was adjusted to pH = 7 using 0.01 N HCl and 0.01N NaOH. The precipitation was centrifuged, rinsed with ethanol, and dried in a vacuum oven.

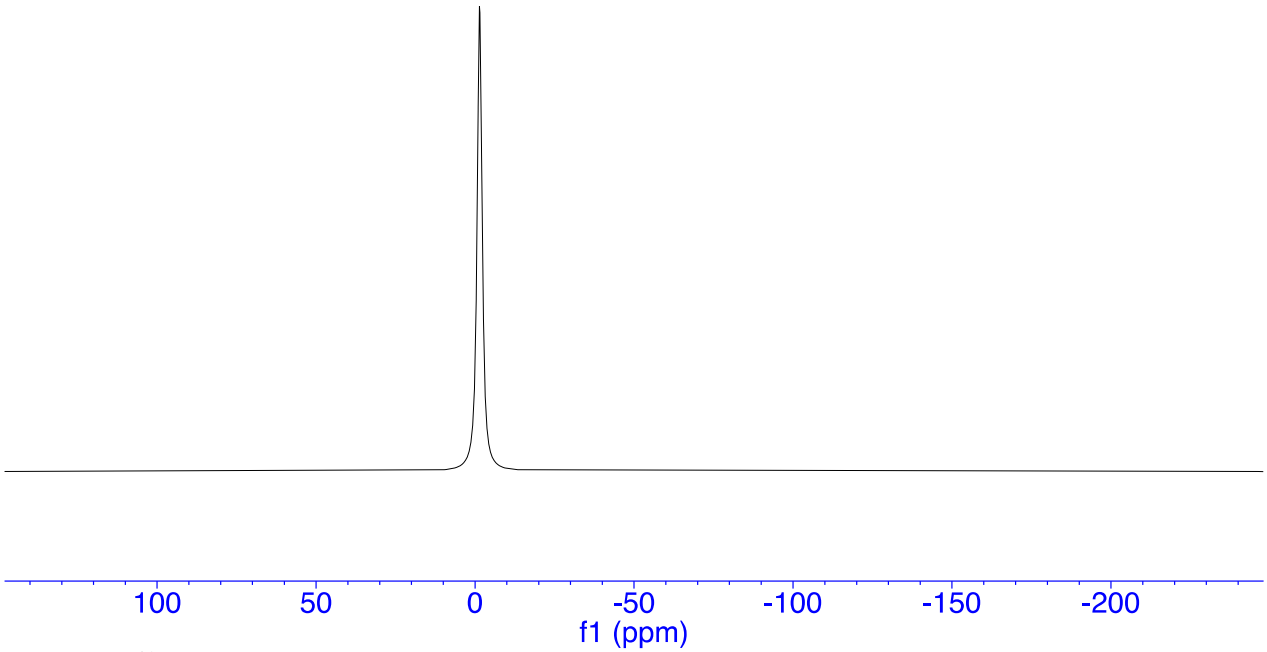

Figure S8. ^{31}P NMR spectrum of of Fe^{III}-HOPO-Pi (DMSO-d_6, 162 MHz). The peak at 0 ppm came from the external reference using: 85% H_3PO_4 diluted to 4% with DMSO.

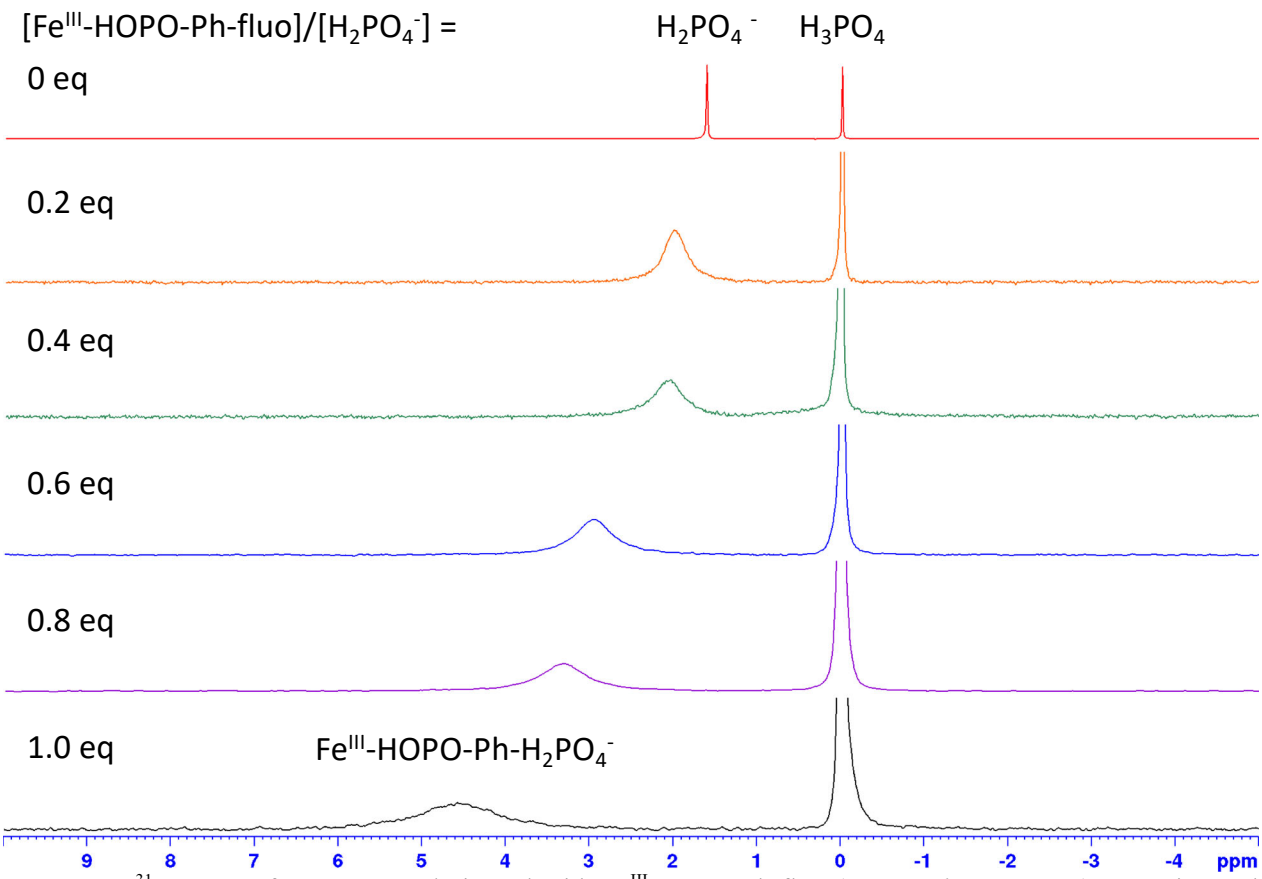

Figure S9. ^{31}P NMR of $Bu_4N{\cdot}H_2PO_4$* titrated with Fe^{III}-HOPO-Ph-fluo (DMSO-d_6, 162 MHz). Experimental conditions: [$Bu_4N{\cdot}H_2PO_4$] = 0.11 M in DMSO-d_6. External reference: 85% H_3PO_4 diluted to 4% with DMSO. *$Bu_4N{\cdot}H_2PO_4$ was used due to the low solubility of inorganic phosphate in DMSO, and low solubility of Fe^{III}-HOPO-Pi in MeOH.

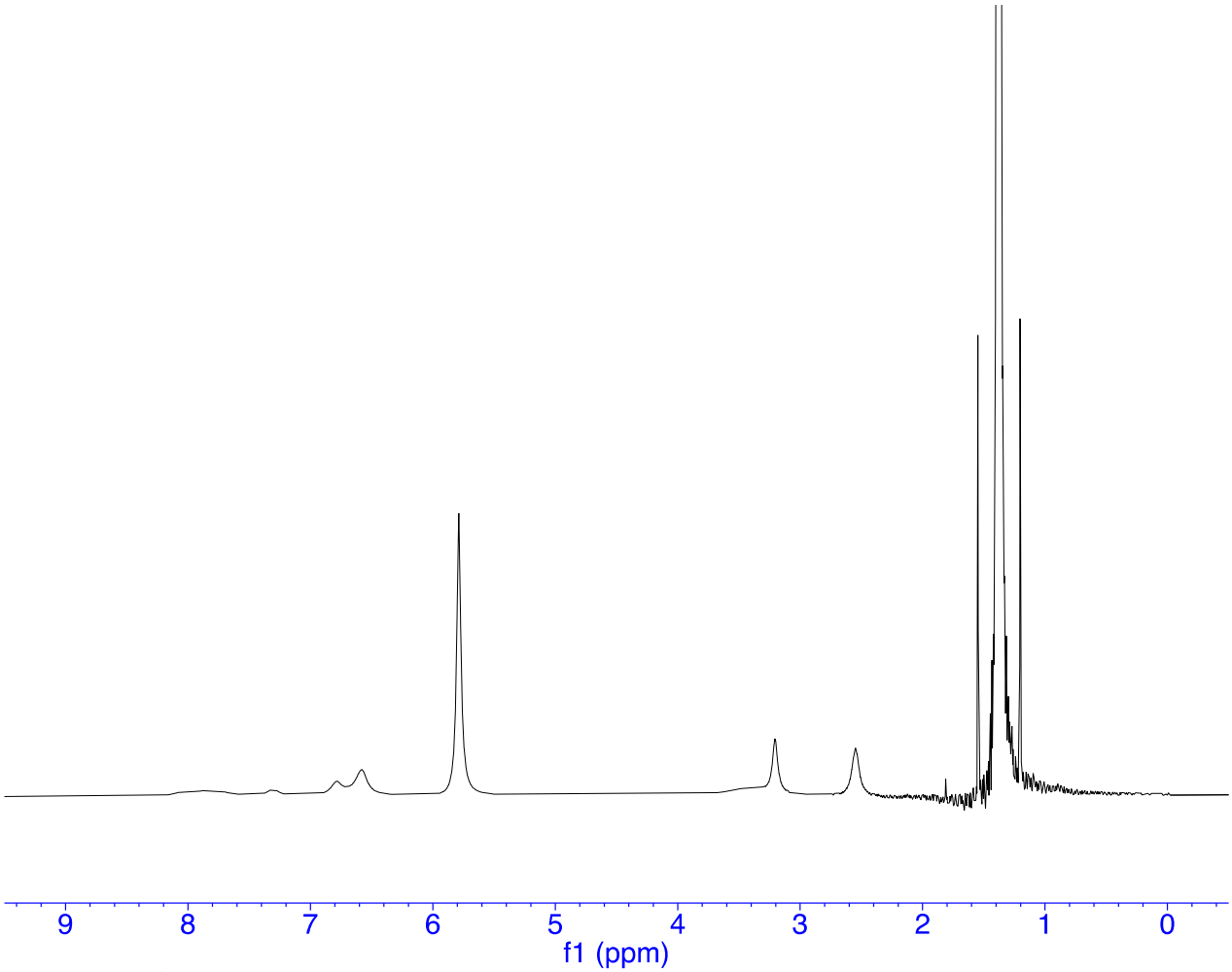

Figure S10. ^{1}H NMR of $Bu_4N{\cdot}H_2PO_4$* titrated with 1 eq. of Fe^{III}-HOPO-fluo+Pi (DMSO-d_6, 162 MHz). Experimental conditions: [$Bu_4N{\cdot}H_2PO_4$] = 0.11 M in DMSO-d_6. External reference: 85% H_3PO_4 diluted to 4% with DMSO. *$Bu_4N{\cdot}H_2PO_4$ was used due to the low solubility of inorganic phosphate in DMSO, and low solubility of Fe^{III}-HOPO-Pi in MeOH.

Job's plot studies

The binding ratios of Fe^{III}-HOPO-fluo + Pi and Fe^{III}-HOPO-PhO-fluo + Pi were estimated by Job's plot studies. Each data point represents the integrated fluorescence emission change with respect to that of same volume of water added in replacement of Pi.

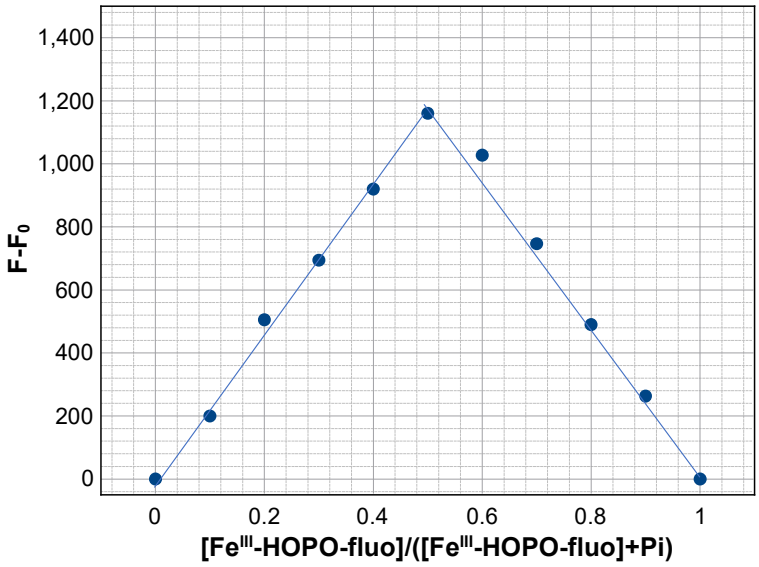

Figure S11. Job's plot analysis of Fe^{III}-HOPO-fluo with phosphate**.** F: integrated luminescence from 500 nm to 650 nm. Conditions: total concentration of Fe^{III}-HOPO-fluo and phosphate was kept at 10 μM. The pH of all solutions was adjusted to 7 using 0.01 N HCl and 0.01 N NaOH. λ_{ex}: 456 nm, excitation and emission slit widths: 5 nm, T = 25°C.

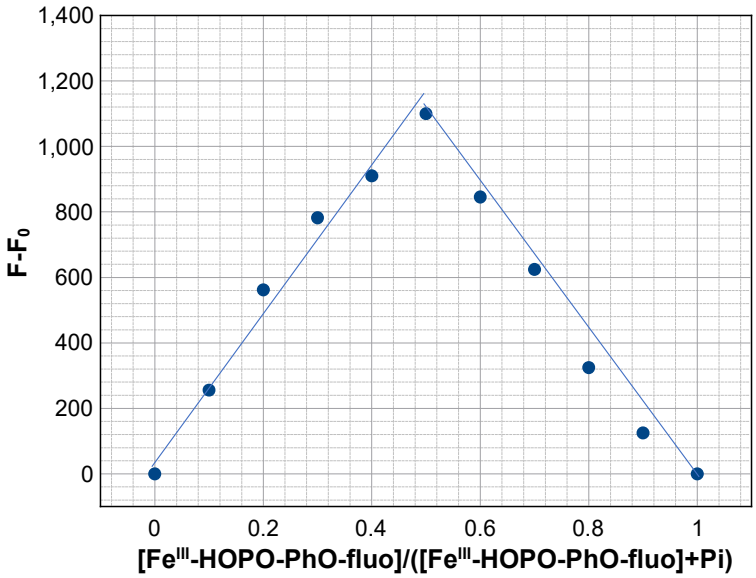

Figure S12. Job's plot of Fe^{III}-HOPO-PhO-fluo with phosphate**.** F: integrated luminescence from 500 nm to 650 nm. Conditions: total concentration of Fe^{III}-HOPO-PhO-fluo and phosphate was kept at 10 μM. The pH of all solutions was adjusted to 7 using 0.01 N HCl and 0.01 N NaOH. λ_{ex}: 456 nm, excitation and emission slit widths: 5 nm, T = 25°C.

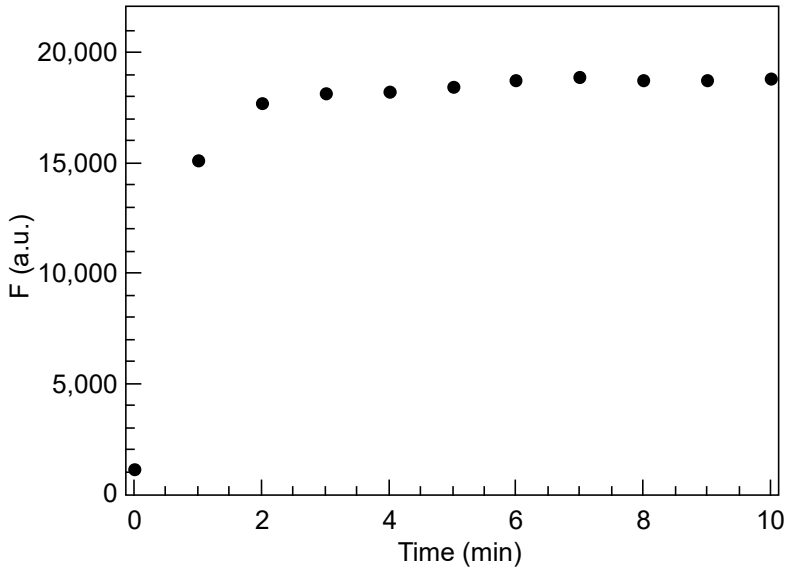

Figure S13. Kinetics of response of Fe^{III}-HOPO-fluo upon addition of phosphate. F: integrated luminescence from 500 nm to 650 nm in the presence of 1 eq. of phosphate. Conditions: [Fe^{III}-HOPO-fluo] = 10 μM in wet ethanol. The pH of all solutions was adjusted to 7. λ_{ex}: 456 nm, excitation and emission slit widths: 5 nm.

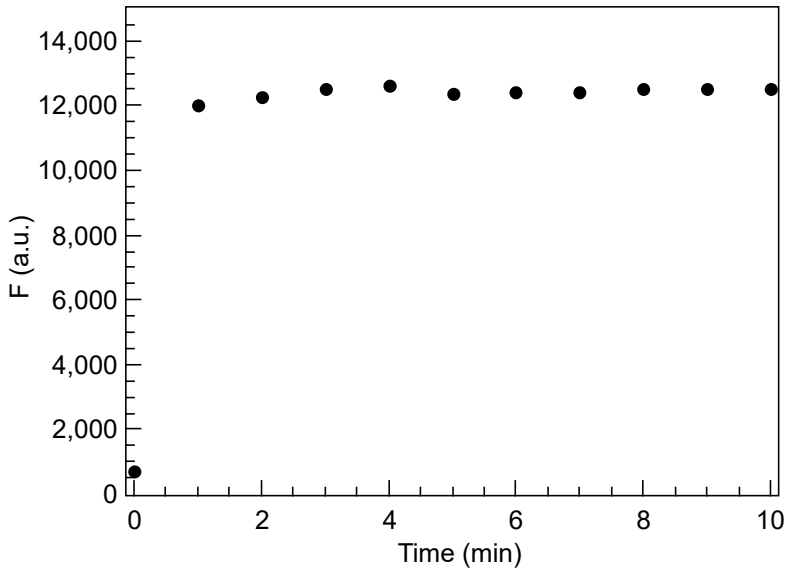

Figure S14. Kinetics of response of Fe^{III}-HOPO-OPh-fluo to phosphate. F: integrated luminescence from 500 nm to 650 nm in the presence of 1 eq. of phosphate. Conditions: [Fe^{III}-HOPO-OPh-fluo] = 10 μM in wet ethanol. The pH of all solutions was adjusted to 7. λ_{ex}: 456 nm, excitation and emission slit widths: 5 nm.

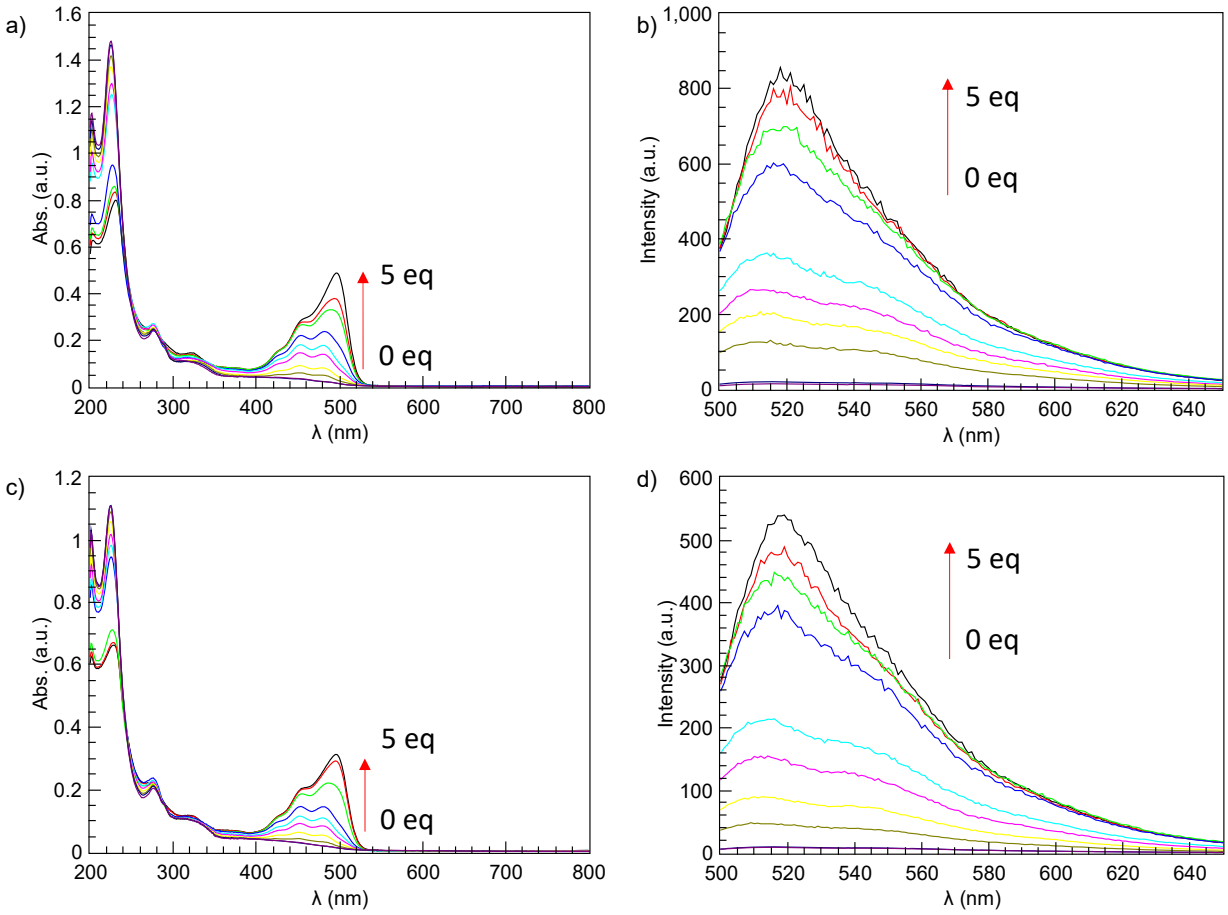

Figure S15. UV-Visible and fluorescence titration spectra of Fe^{III} complexes with phosphate: a) UV-Visible spectra of Fe^{III}-HOPO-fluo with phosphate; b) fluorescence spectra of Fe^{III}-HOPO-fluo with phosphate; c) UV-Visible spectra of Fe^{III}-HOPO-PhO-fluo with Pi; d) fluorescence spectra of Fe^{III}-HOPO-PhO-fluo with phosphate. Conditions: [Fe^{III}-HOPO-fluo] and [Fe^{III}-HOPO-PhO-fluo] = 10 µM in wet ethanol. pH = 7. λ_{ex}: 456 nm, excitation and emission slit widths: 5 nm.

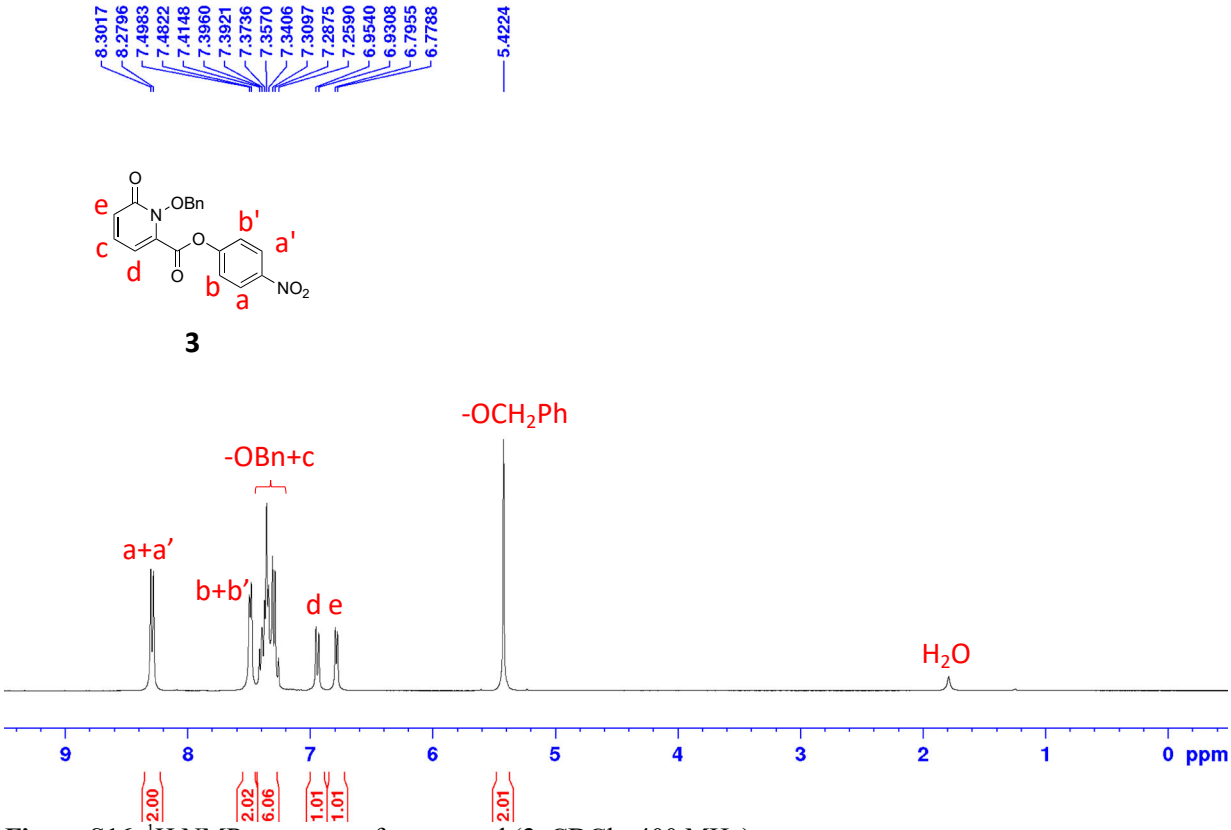

Figure S16. ^{1}H NMR spectrum of compound (**3**, $CDCl_3$, 400 MHz).

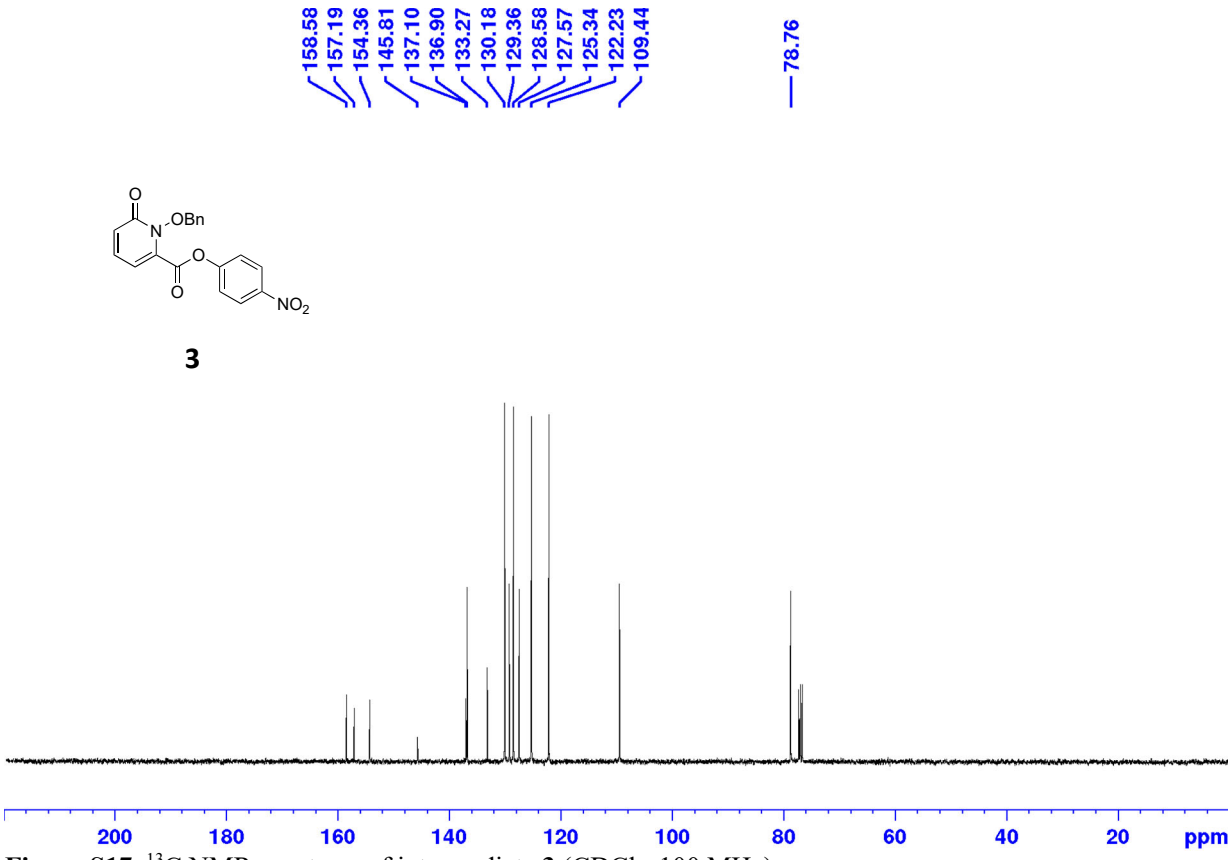

Figure S17. ^{13}C NMR spectrum of intermediate **3** ($CDCl_3$, 100 MHz).

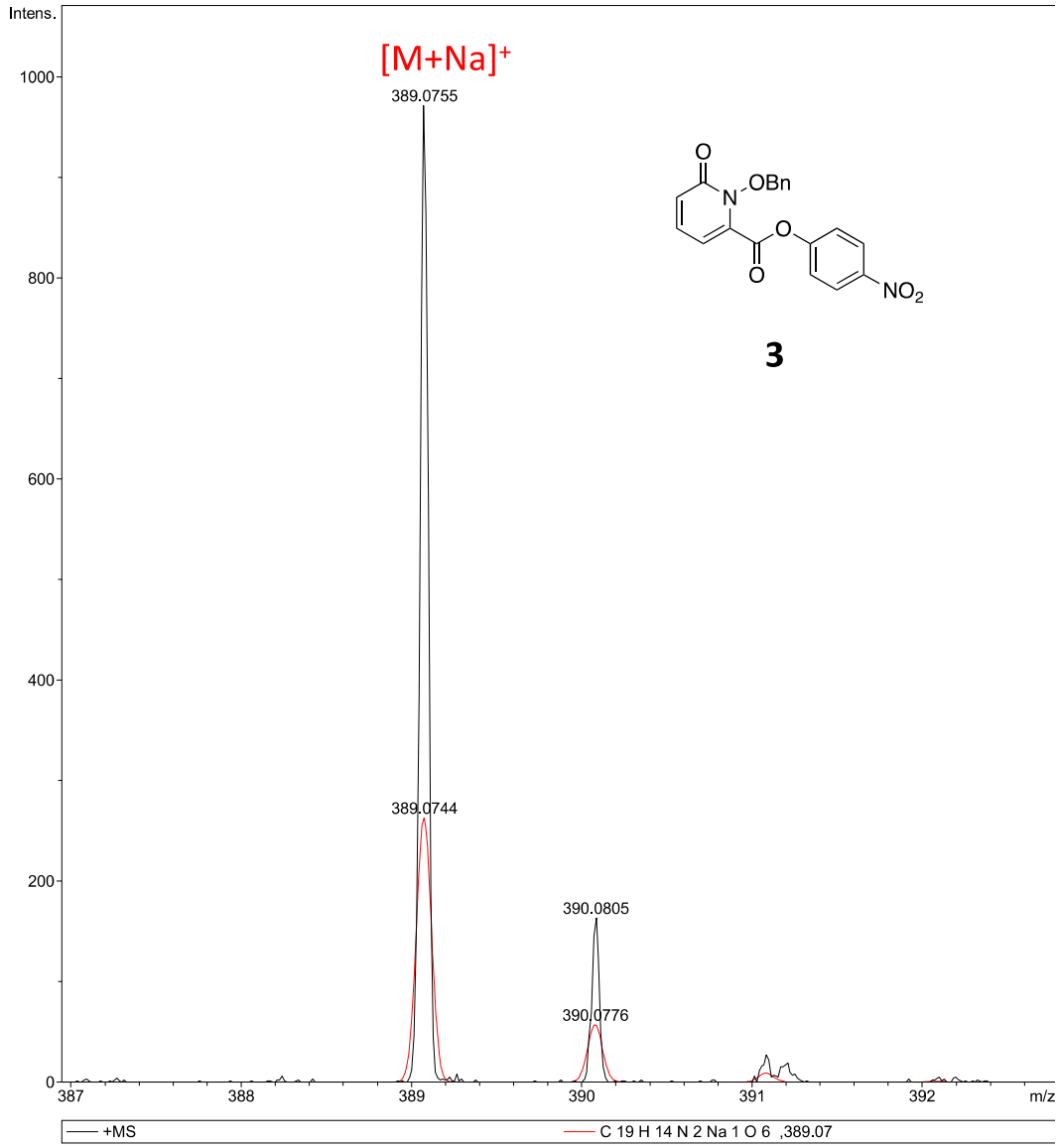

Figure S18. Experimental (black) and calculated (red) ESI-MS spectrum of intermediate **3**.

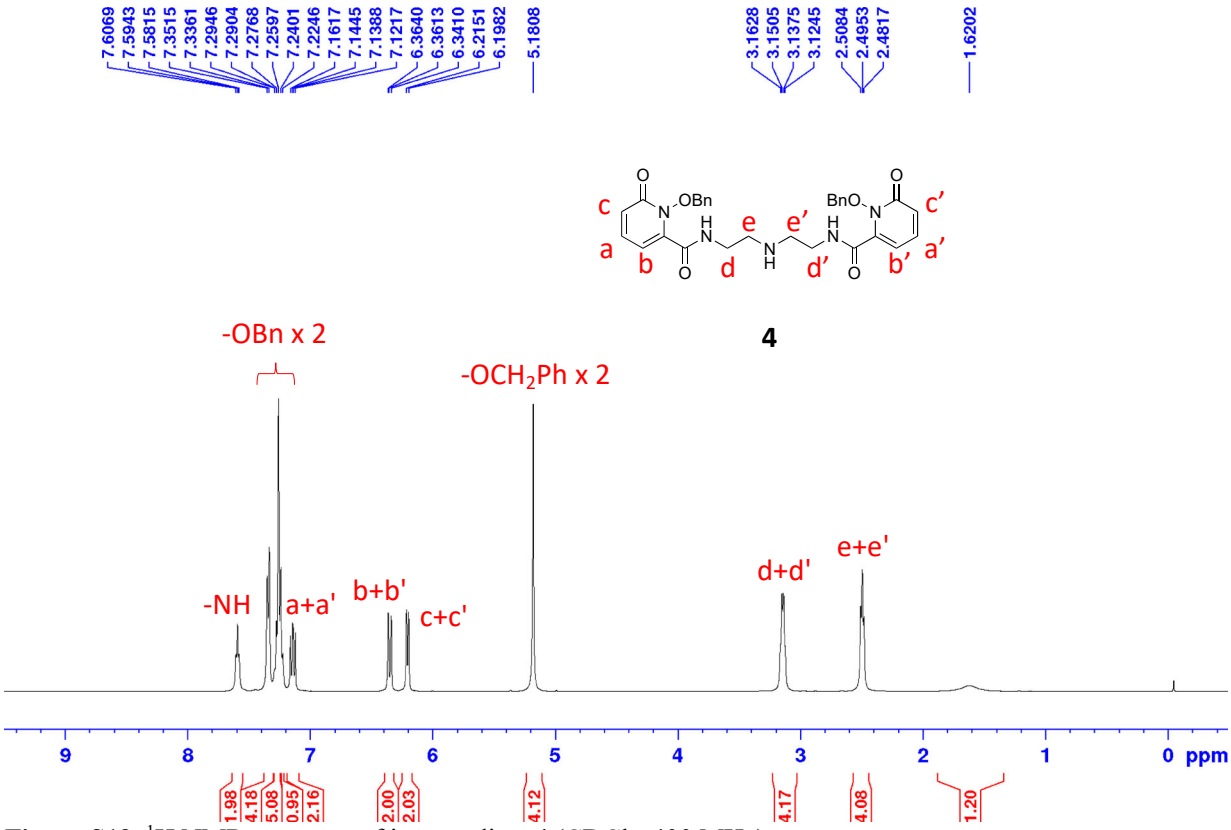

4

Figure S19. ^{1}H NMR spectrum of intermediate **4** ($CDCl_3$, 400 MHz).

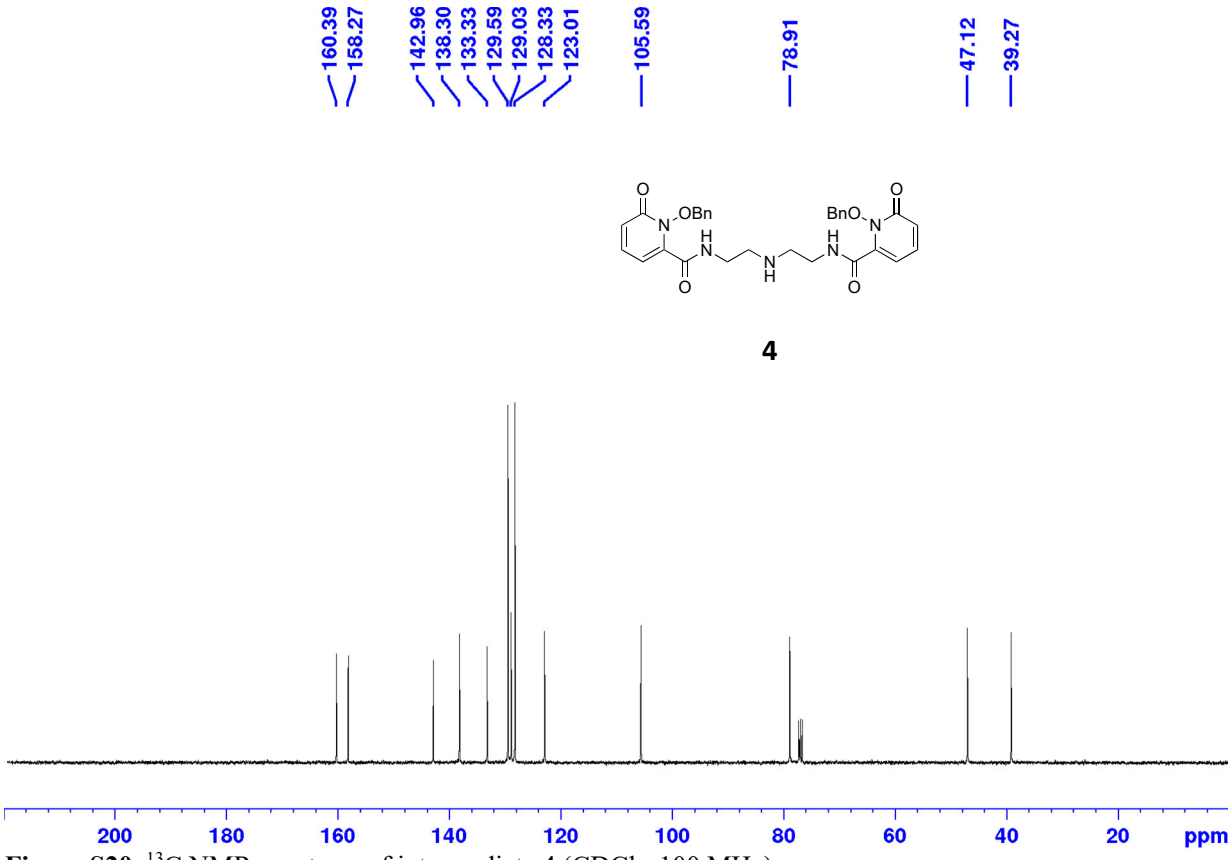

4

Figure S20. ^{13}C NMR spectrum of intermediate **4** ($CDCl_3$, 100 MHz).

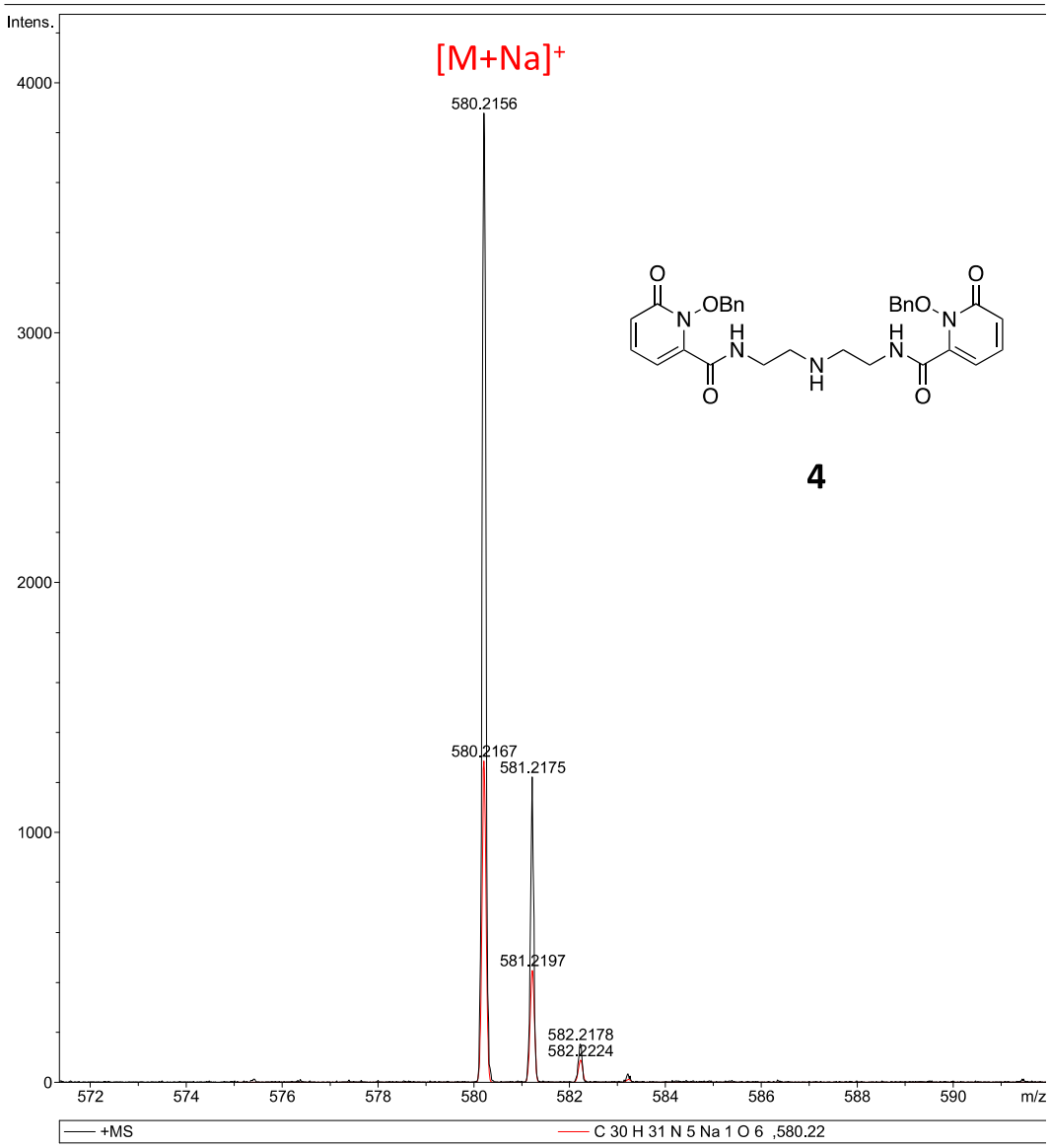

Figure S21. Experimental (black) and calculated (red) ESI-MS spectrum of intermediate **4**.

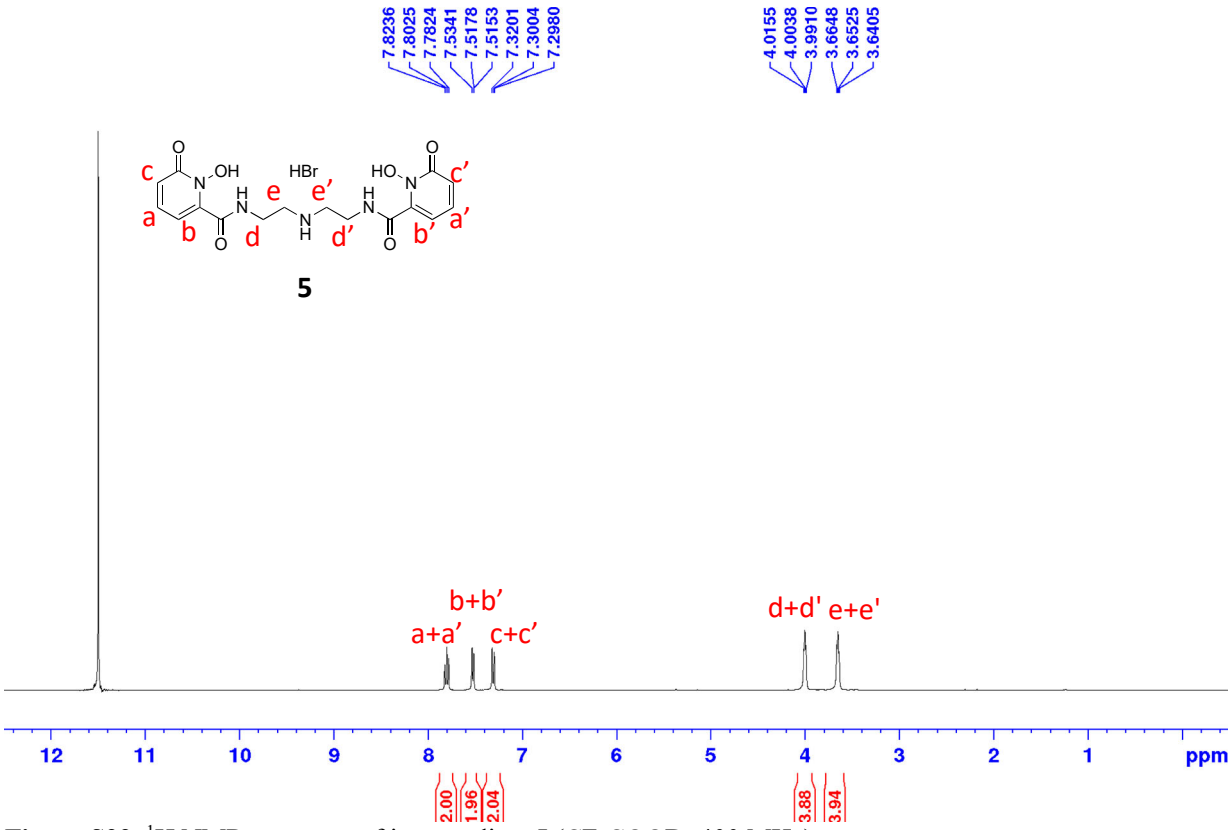

Figure S22. ^{1}H NMR spectrum of intermediate **5** (CF_3COOD, 400 MHz).

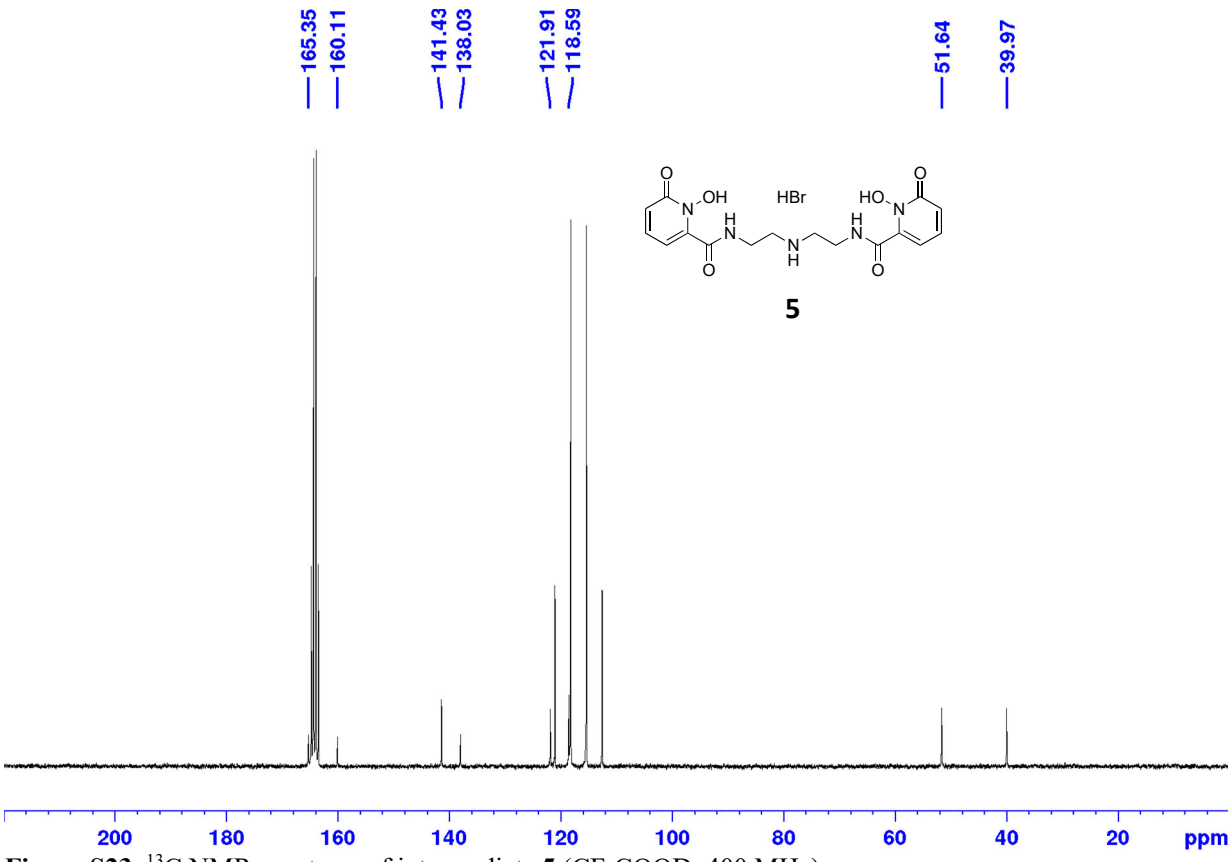

Figure S23. ^{13}C NMR spectrum of intermediate **5** (CF_3COOD, 400 MHz).

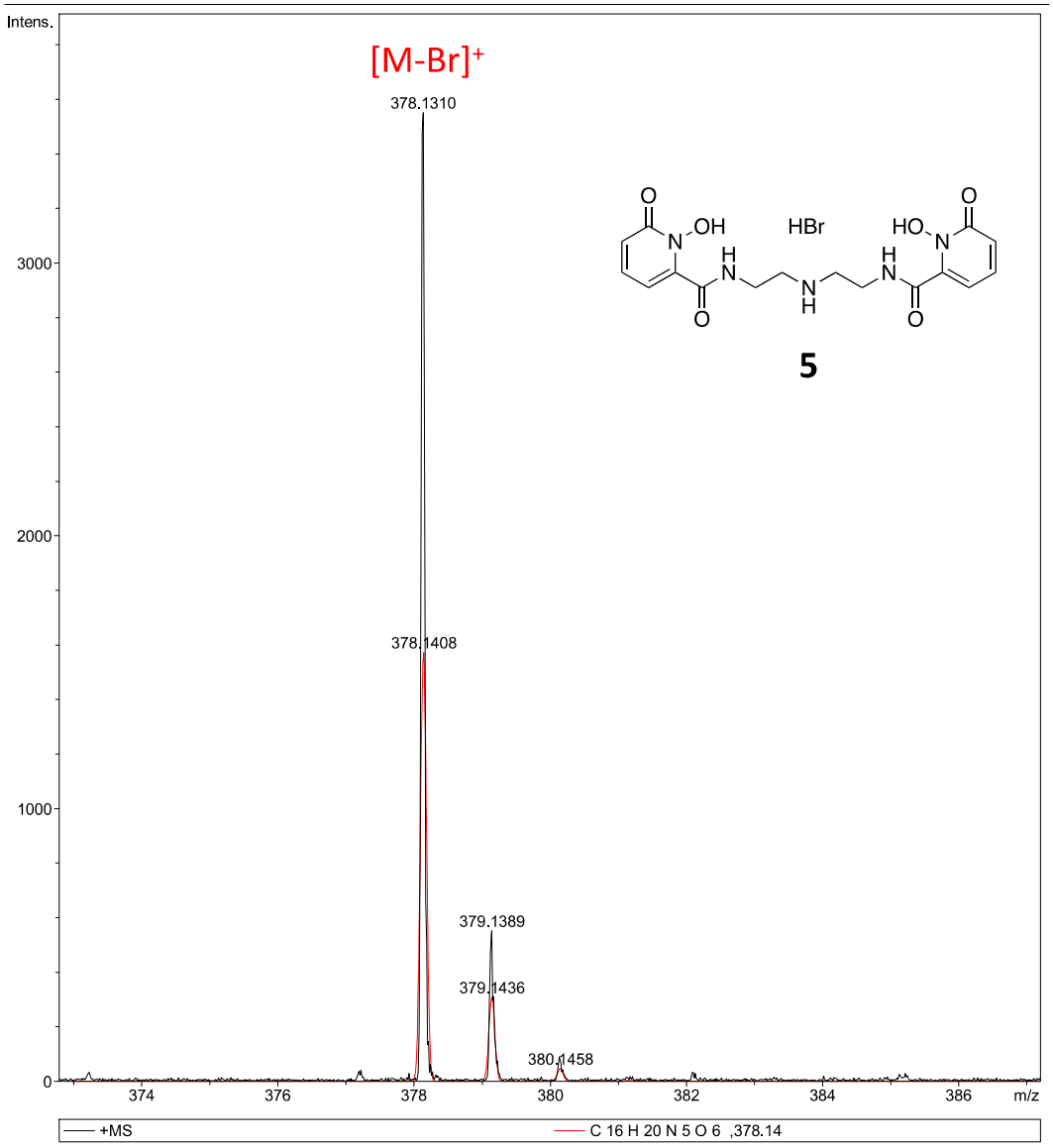

Figure S24. Experimental (black) and calculated (red) ESI-MS spectrum of intermediate **5**.

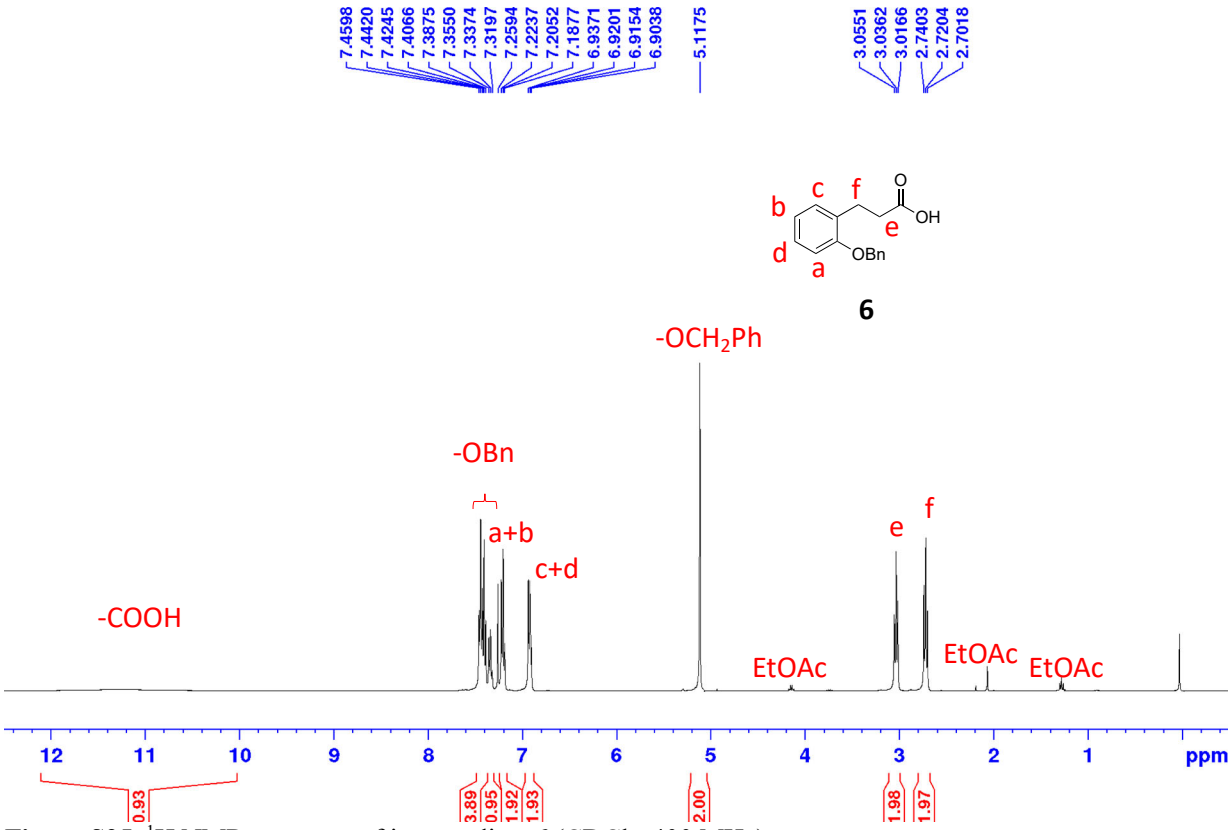

Figure S25. ^{1}H NMR spectrum of intermediate **6** ($CDCl_3$, 400 MHz).

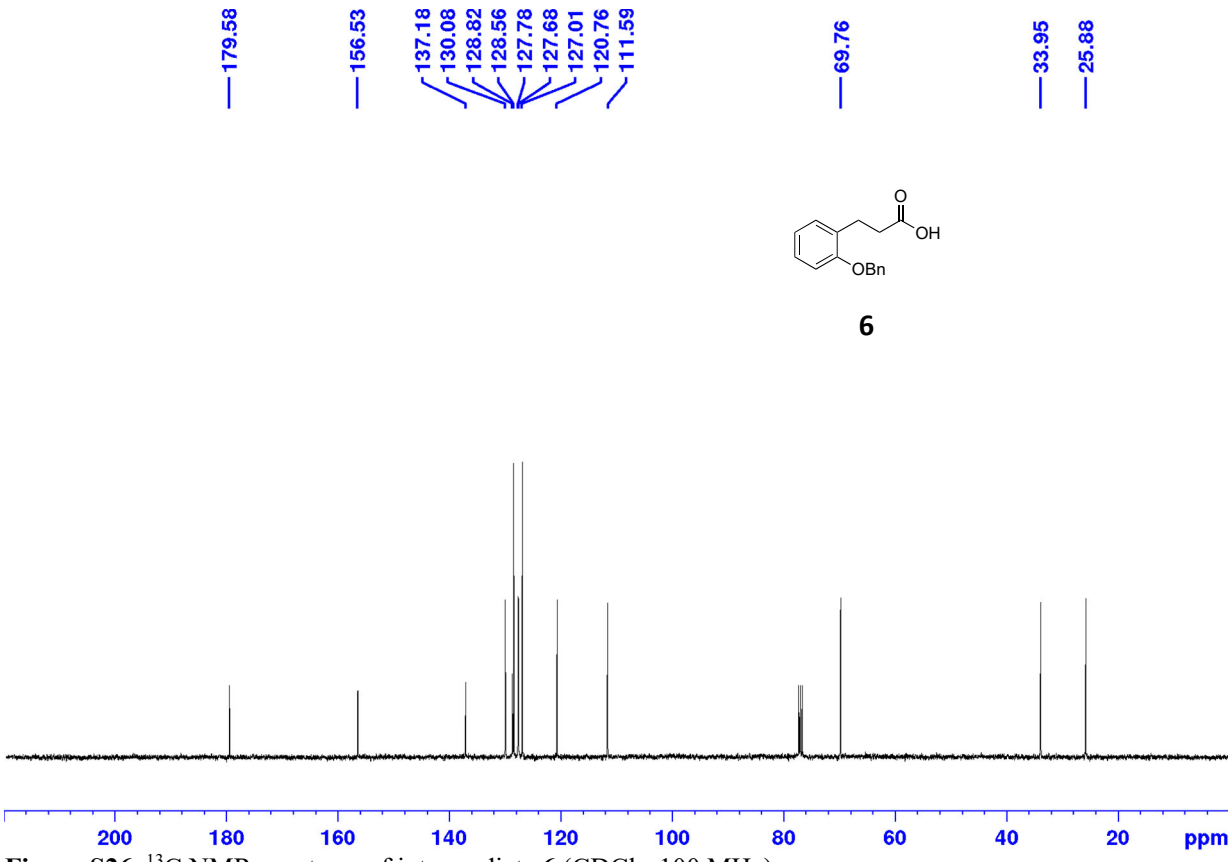

Figure S26. ^{13}C NMR spectrum of intermediate **6** ($CDCl_3$, 100 MHz).

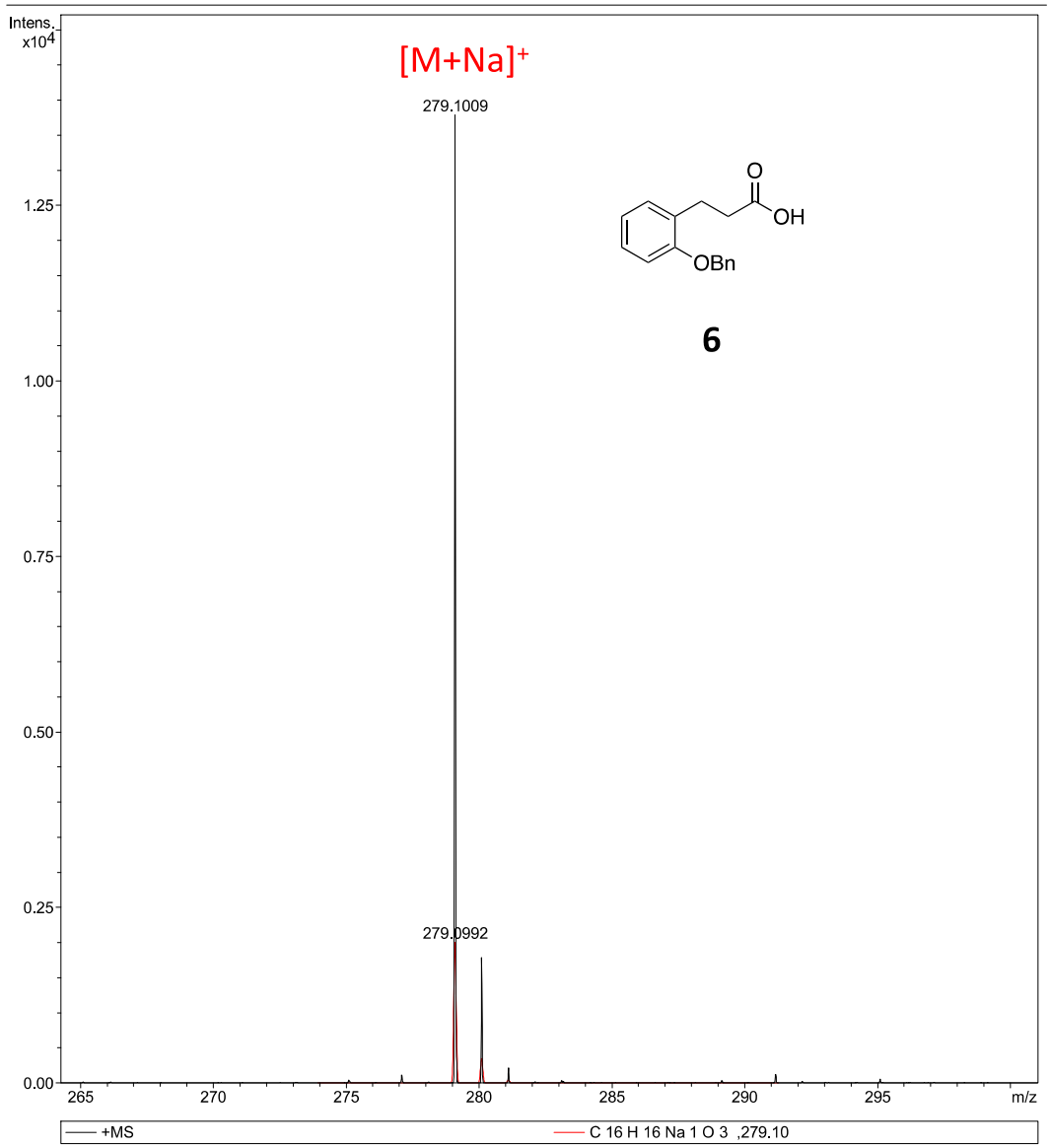

Figure S27. Experimental (black) and calculated (red) ESI-MS spectrum of intermediate **6**.

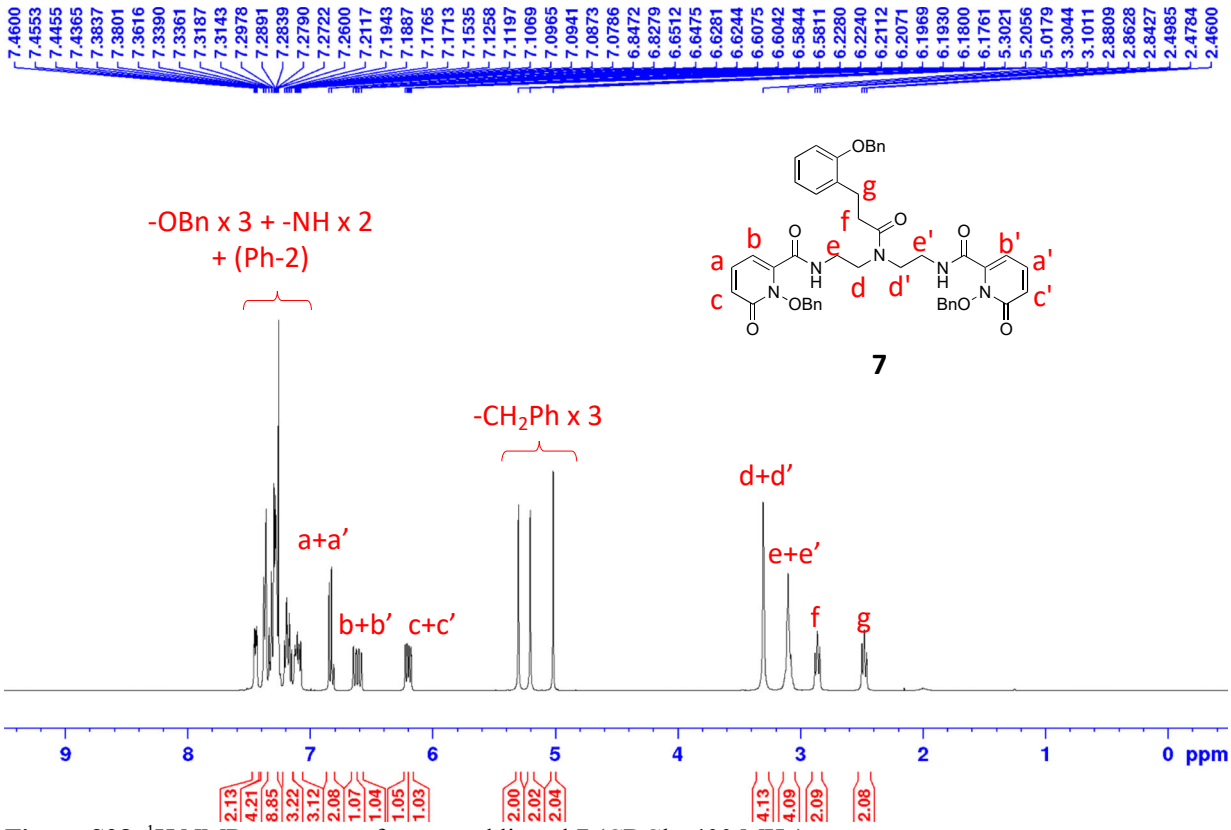

Figure S28. ^{1}H NMR spectrum of protected ligand **7** ($CDCl_3$, 400 MHz).

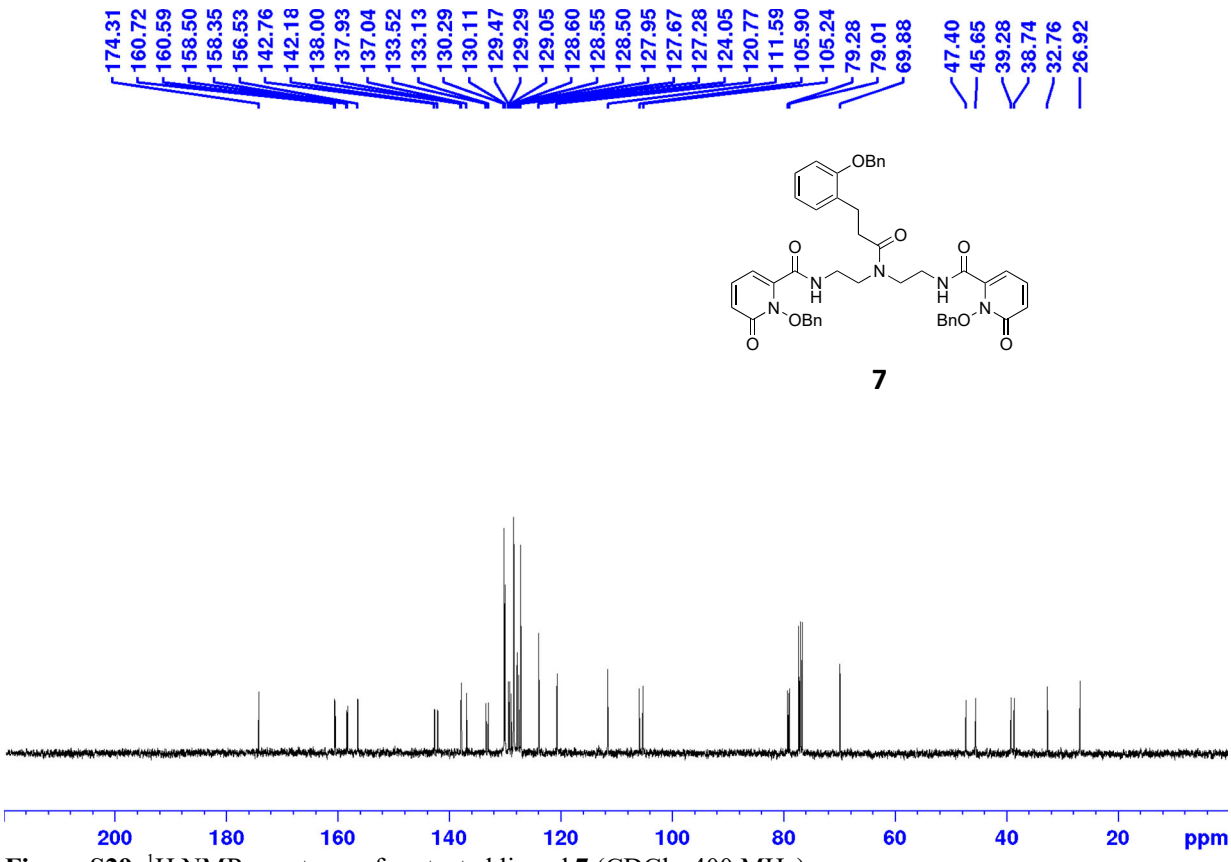

Figure S29. ^{1}H NMR spectrum of protected ligand **7** ($CDCl_3$, 400 MHz).

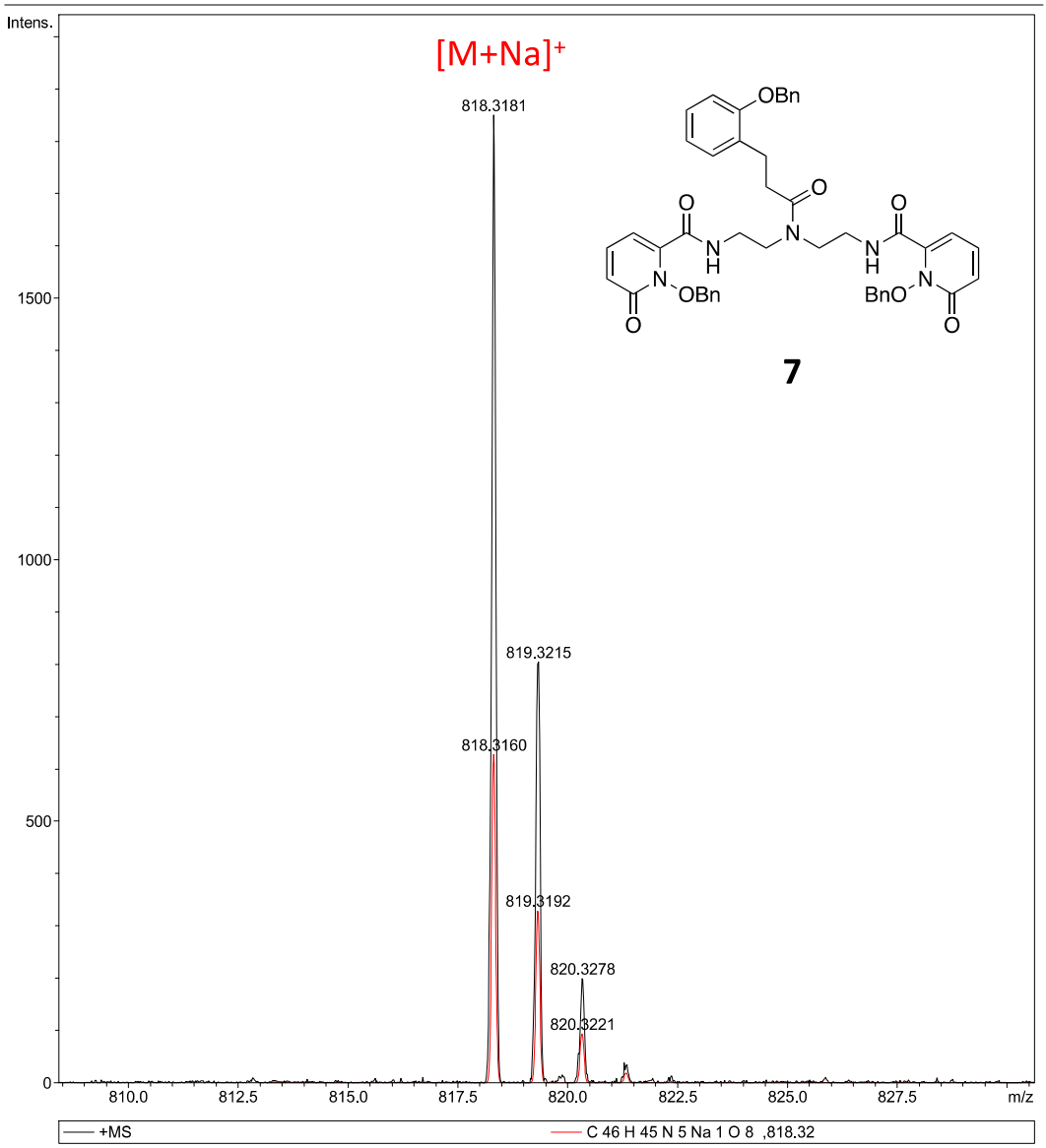

Figure S30. Experimental (black) and calculated (red) ESI-MS spectrum of protected ligand **7**.

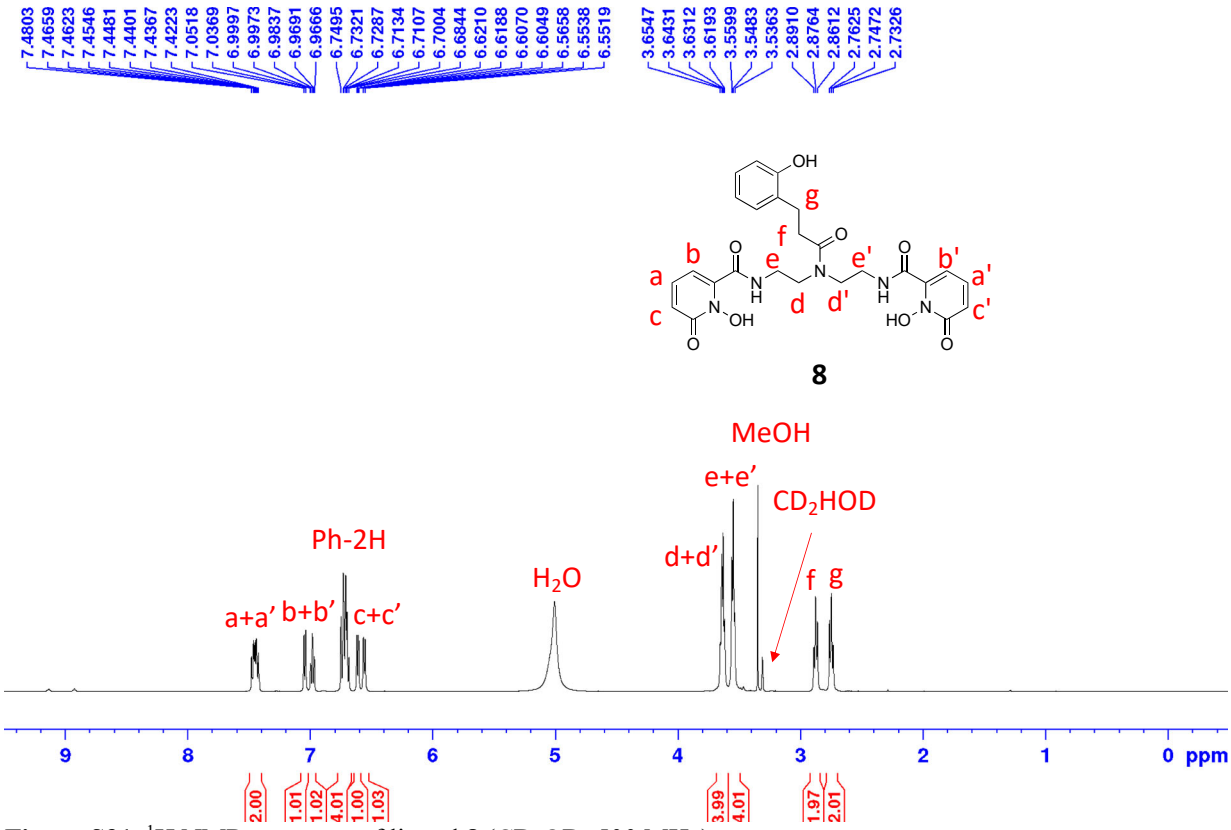

Figure S31. ^{1}H NMR spectrum of ligand **8** (CD_3OD, 500 MHz).

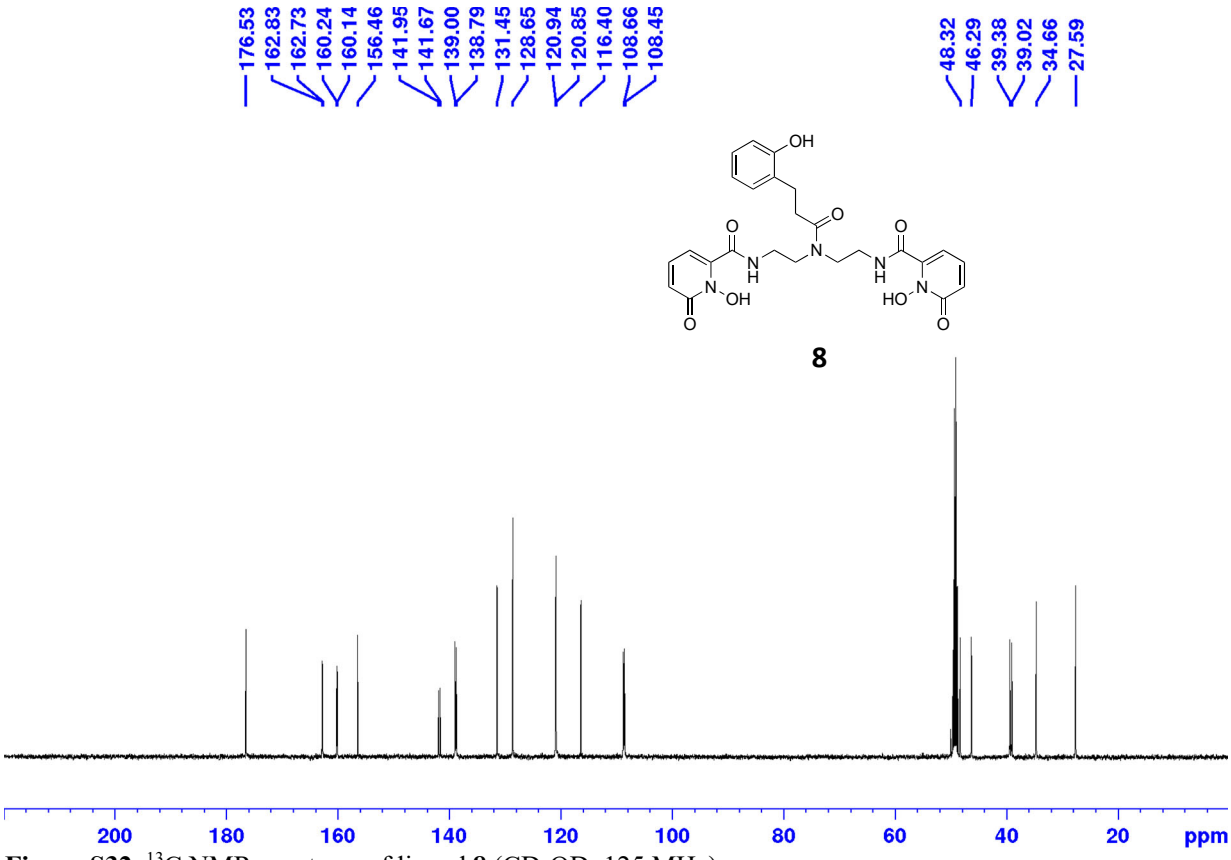

Figure S32. ^{13}C NMR spectrum of ligand **8** (CD_3OD, 125 MHz).

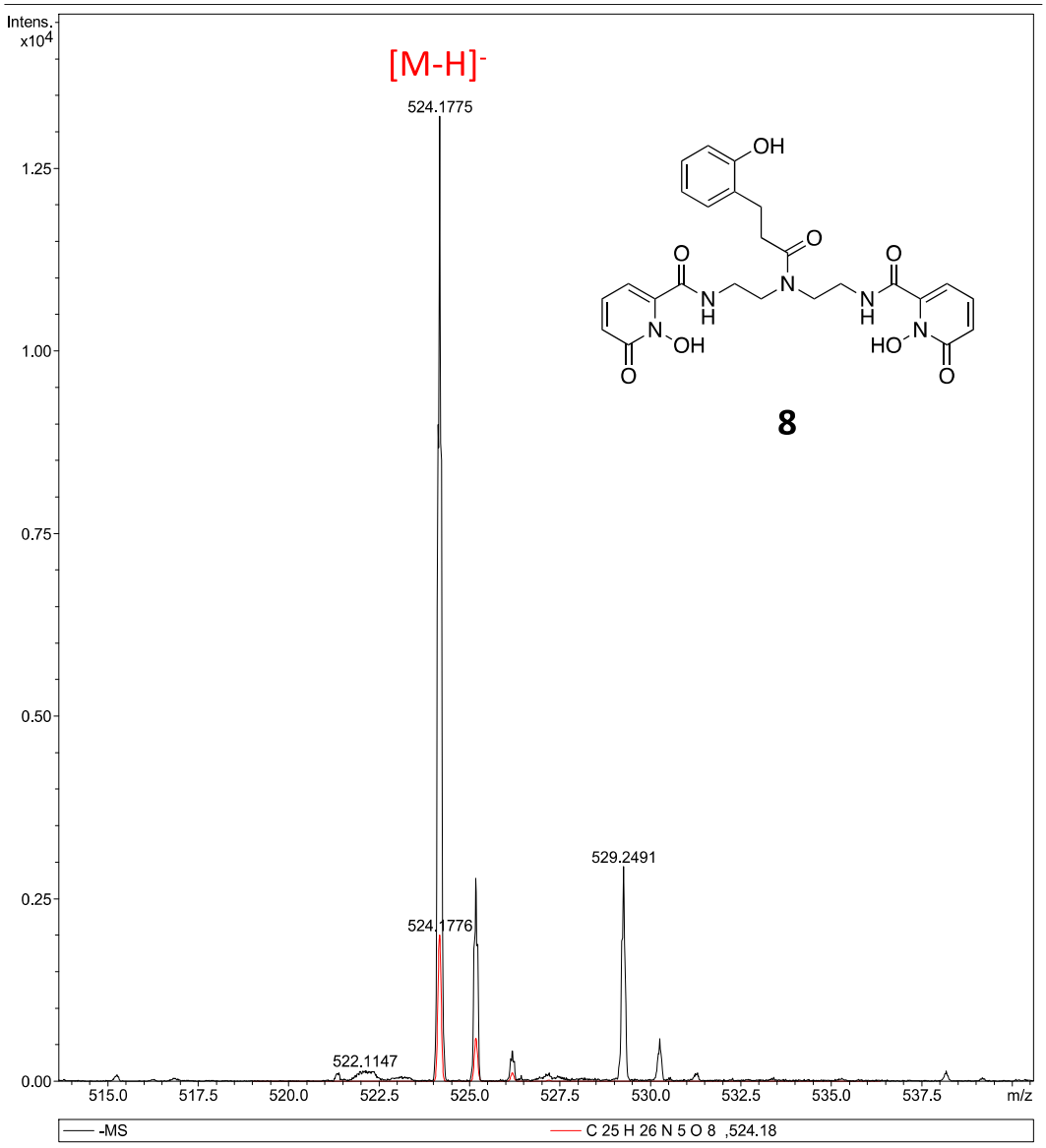

Figure S33. Experimental (black) and calculated (red) ESI-MS spectrum of ligand **8**.

Data fitting

Data fitting of Fe^{III}-complexes + Pi uses the following equations:

$$[H] + [G] \rightleftharpoons [HG]$$

where H denotes the host (Fe^{III}-complex-fluo), G the guest (Pi), and HG the adduct. Equilibrium constants K is defined as:

$$K = \frac{[HG]}{[H][G]}$$

The luminescence intensity increase can be described as the following:[2]

$$F - F_0 = \frac{1}{2[H]_0}\Delta F_{Max}\{[G]_0 + [H]_0 + \frac{1}{K} - \sqrt{([G]_0 + [H]_0 + \frac{1}{K})^2 - 4[G]_0[H]_0}\}$$

where

F = integrated fluorescence,

F_0 = initial integrated fluorescence,

$\Delta F_{max} = F_\infty - F_0$.

Non-linear fitting was performed using QtiPlot 1.0.0 software.

Detection limits were calculated according to 3σ, where σ is the standard deviation of the fitting.

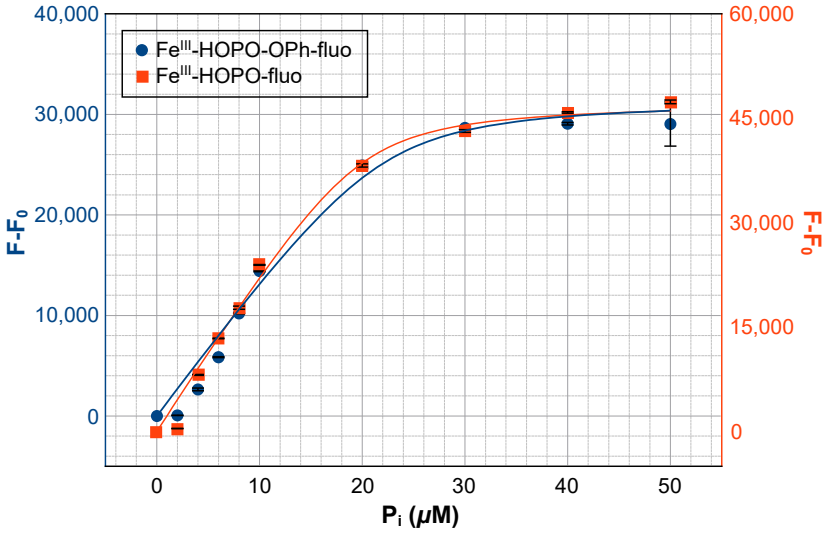

Fitting results:

Table S1. Fitting results of Fe^{III}-HOPO-fluo+Pi and Fe^{III}-HOPO-OPh-fluo+Pi.

	K (M^{-1})	R^2	σ
Fe^{III}-HOPO-OPh-fluo	$8.8 \pm 3.4 \times 10^5$	0.982	1665
Fe^{III}-HOPO-fluo	$1.1 \pm 0.5 \times 10^6$	0.992	1737

References

[1] F. Guérard, M. Beyler, Y.-S. Lee, R. Tripier, J.-F. Gestin, M. W. Brechbiel, *Dalton Trans.* **2017**, *46*, 4749–4758.
[2] K. L. Amsberry, R. T. Borchardt, *J. Org. Chem.* **1990**, *55*, 5867–5877.